TECHNICAL NOTES

NATIONAL ADVISORY COMMITTEE FOR AERONAUTICS

NO. 922

OVALIZATION OF TUBES UNDER BENDING AND COMPRESSION

By L. J. Demer and E. S. Kavanaugh
University of Notre Dame

Washington
March 1944

NATIONAL ADVISORY COMMITTEE FOR AERONAUTICS

TECHNICAL NOTE NO. 922

OVALIZATION OF TUBES UNDER BENDING AND COMPRESSION

By L. J. Demer and E. S. Kavanaugh

SUMMARY

An empirical equation has been developed that gives the approximate amount of ovalization for tubes under bending loads. Tests were made on tubes in the D/t range from 6 to 14, the latter D/t ratio being in the normal landing gear range. Within the range of the series of tests conducted, the increase in ovalization due to a compression load in combination with a bending load was very small, the bending load being the principal factor in producing the ovalization. The ovalization is a rather complex function of the bending moment, D/t ratio, cantilever length, and distance between opposite bearing faces.

INTRODUCTION

This investigation was proposed because it has been found that the cantilever landing struts on large airplanes fail to telescope properly when they are subjected to side loads. This "freezing" of the strut seriously impairs the shock absorption of the landing gear. The failure of the strut to telescope properly has been attributed to the ovalization of the piston when the side load is applied, and the aim of this investigation has been to measure this change in diameter of the strut and to arrive at a satisfactory equation for calculating the increase in diameter. As far as the authors have determined, no previous investigation has been made of the ovalization produced by this type of loading.

This investigation was conducted in the laboratories of the University of Notre Dame under the supervision of Prof. F. N. M. Brown. The funds were provided by the National Advisory Committee for Aeronautics and the specimens and photographs were supplied by the Bendix Products Division of South Bend, Indiana.

SYMBOLS

M	cantilever bending moment, inch-pounds
D	outside diameter of tube, inches
t	wall thickness of tube, inches
w	ovalization, inches
L	cantilever length of tube, inches
J	distance between opposite bearing faces, inches

DESCRIPTION OF APPARATUS

The apparatus and method of loading the test specimen are shown in figures 1, 2, and 3. The support, for the bearings and loading apparatus, consisted of a beam made of two 18-inch steel channels bolted together by means of steel plates on top and bottom. This beam was supported by four screw jacks mounted on each corner of the beam. A fixed bearing was welded to one end of the channels to form one end support for the tube to be tested and a movable bearing was mounted on the top of the channels to form the second support. The load was applied at the end of the tube opposite the fixed bearing. A portable hydraulic jack was used to apply the bending load to the tube, a cradle type yoke being used between the tube and the base of the jack, as shown in figure 3. A Bourdon type pressure gage was inserted in the hydraulic line of the jack and was used to determine the load applied; the gage was calibrated, and the load read from a curve of load vs. pressure. A similar cradle was used to apply a compression load (fig. 3b) on the tube through the use of another hydraulic jack, similarly calibrated.

Several types of deflection gages were tested before the final gage was decided upon. Two types are shown in figures 4 and 5; the latter type, figure 5, is the one with which the most success has been obtained. Figure 4 shows the parallel-arm type gage which was used for the tests made on the largest tube (diameter 4.610") and on the second tube (diameter 4.375"). A complete set of

readings was also taken with the second type, the double-indicator gage, on the 4.375 inch diameter tube. The deflections indicated by the two types agreed quite closely, but the second type gage was more easily assembled and is believed to be more reliable. The double-indicator gage gave direct readings while the parallel-arm type gave magnified readings which had to be corrected. The double-indicator type gage was supported on the tube by four pointed setscrews, the screws being 90° apart and in contact with the tube at points where the deflection was either zero or small negatively. The indicators used for measuring the deflection were of the Jordan type and were graduated in ten-thousandths of an inch.

An inside gage consisting of a single Jordan type indicator, mounted so that it measured the change in the inside diameter at the 90° azimuth, was used for tubes of 4.251 inch diameter and less. The plane in which the applied load acts was taken as the 0° azimuth, making the 90° azimuth the plane of the neutral axis of the tube. The readings obtained with this gage were not very reliable, but they did indicate that the maximum ovalization occurred very near station 0 (plane of the face of the movable bearing on the side of the applied load) as long as the ovalization did not exceed the bearing clearance.

DESCRIPTION OF TEST ARTICLES AND METHODS OF PERFORMING TESTS

The test specimen used was made from an SAE X-4130 tube. The original diameter and wall thickness of the tube was 4-5/8 inches outside diameter × 3/4 inch wall. The over-all length of the test specimen was 47 inches. Tensile specimens tested in the University laboratories indicated the ultimate tensile strength to be 147,500 lb/in.^{2}, and the yield point to be 117,500 lb/in.^{2}. The Brinell hardness number was about 347. The bearings for the two supports were made from an SAE 1020 tube. A heavy sleeve was fitted over the end of the test specimen in such a manner as to make the distance from the centerline of the fixed bearing to the centerline of the applied load 55-1/16 inches. For details of the test setup, see figures 1 and 2.

The range of D/t ratios, 6 to 14, that was tested

was obtained by reducing the outside diameter of the test specimen after the series of tests had been conducted at one D/t ratio. The inside diameter of the tube was held constant at 3.125 inches. Tests were conducted with outside diameters of 4.610, 4.375, 4.251, 3.929, and 3.650 inches. In each case, the outside was ground concentric with the inside.

The outside diameters of the tube were held to a tolerance of ±0.001. The bearing clearance was held between 0.0020 and 0.0040 inch over the outside diameter of the tube. This clearance was designed to stay within the allowable bearing clearances specified for actual landing gears.

The first tests were made to determine the points on the tube where the increase in diameter of the tube was the greatest, as it was at this point that the tube would tend to "freeze" in the bearing if the ovalization became great enough. The axial location of points at which the measurements were taken are designated by inch stations, using the plane of the face of the movable bearing on the side of the applied load as the zero reference station. (See fig. 2.) The stations between the reference station and the applied load are considered positive. Measurements were taken at various stations along the length of the tube from the fixed bearing to station plus 10 inches. The measurements at each station were taken around the circumference of the tube, using the vertical centerline of the tube as the reference point, zero azimuth. Azimuth readings were taken at 15° increments.

Six bearing positions, A, B, C, D, E, and F, as shown in figure 2, were used during the investigation, the ratio of tube length to the distance between bearings varying between 15.3 and 2.4. In this case the length of tube is considered to be the distance (55-1/16 in.) between the centerline of the fixed bearing and the applied load and the distance between bearings to be the distance between their centerlines. In all other places in this report the distance between bearings is considered to be the distance between opposite bearing faces (J). This criterion was chosen because the distance between opposite bearing faces is a standard designation in strut design specifications. The six values of J used in this investigation were 7.12, 12.75, 17.36, 21.97, 26.58 and 31.19 inches. The bearing position distances for positions B through F vary by increments that are multiples of the original diameter of the tube, 4.610 inches.

The gages used for measuring ovalization were alined on the tube by scaling the distance from the zero reference station to the centerline of the leg of the dial gage and placing in the correct azimuth by use of a level bubble and a square. The gage was then fastened to the tube so that it supported itself.

Before beginning a test a comparatively heavy load of about 4,000 pounds was applied to the tube in order to check the gage for proper alinement. The number and magnitude of the bending loads applied varied with the bearing position and tube diameter. A low load was first applied and then increased in predetermined steps until the maximum load was reached, the reading of the dials of the gage being recorded as each load was applied. At least two sets of readings were taken at each station as a check.

The tests to determine the effect of a compression load on ovalization were made with and without bending loads, the ovalization gage being alined in the same manner as for the tests involving bending loads only. The compression load was applied at the centerline of the tube (see fig. 3b) for one series of tests with and without a bending load and another series of tests with and without a bending load were made with the compression load being applied eccentrically, 4 inches below the centerline of the tube.

The end deflection of the tube was measured for each test and was used to check the applied bending load. The hydraulic gages used in applying the bending load were checked periodically.

The gages used to measure the ovalization were graduated to one-ten-thousandth of an inch. Repeated tests were made at various stations along the tube and such tests indicated that the accuracy of the measurement was within four-ten-thousandths, and it was not unusual for the repeated points to fall within one-ten-thousandth of the original test.

The gages used to measure the oil pressure in the hydraulic jacks were calibrated to read within 30 pounds of the true load.

The complete data gathered during this investigation may be obtained on loan from the Office of Aeronautical Intelligence of the National Advisory Committee for Aeronautics, Washington, D. C.

RESULTS AND DISCUSSION

Numerous measurements were made to determine the amount of ovalization as the circumference of the tube was traversed and figures 7 through 10 show some results of these tests. Measurements were taken of the ovalization of the tube at 15° increments from 0° azimuth to 180° azimuth for the test on the original tube only. All test results are not included in this report, as the tests were made to find the azimuth at which maximum positive ovalization occurred so that later measurements could be concentrated on this one azimuth. This point was found to be the 90° azimuth point. After the first tests, measurements were taken only at 0° and 90° azimuths. The 0° azimuth readings were taken only as a matter of record, as they were not considered as a part of this particular study.

One interesting feature brought out in figures 9 and 10 is that the axis of symmetry shifts downward as the bearing face, or zero reference station, is approached. The curve of the ovalization around the circumference of the tube closely approaches that of a sine curve.

Tests were conducted to determine the point of maximum ovalization along the length of the tube. The results of these tests, as shown in figures 11 and 12, clearly indicate that this point was at the zero reference station.

The longitudinal and circumferential tests discussed above were made with the movable bearing placed at positions B, C, D, and E, although only the data from the tests with position C are included herein.

Figures 13, 14, 15, 16, and 19 are typical plots for one bearing position (position C) of the bending moment at the various stations against ovalization for the range of D/t ratios that were tested, while figures 17 through 22 are typical plots for one D/t ratio (O.D. = 3.650 in.) for the bending moment at the various stations against ovalization for the different bearing positions that were used during the tests. The bending moment is taken as the product of the load and the distance from the station of measurement to the centerline of the applied load, this distance for station zero (0) and the final equation is the lever arm, L, as shown in

figure 1. As the D/t ratio increases the ovalization vs. bending moment curves change from straight lines to smooth curves and finally into a type of curve that has a sharp knee in it (O.D. = 3.650 in.). The bearing clearance for the tubes with diameters of 4.610 inches and 4.251 inches was approximately 0.004 inch. The tube with a diameter of 4.375 inches had a bearing clearance of approximately 0.010 inch. This clearance exceeds the normal landing gear bearing clearance. The 3.929 inch and 3.650 inch diameter tubes had clearances of 0.003 and 0.0025 inch, respectively.

The second series of figures, 23 through 32, are typical plots of ovalization against distance from the bearing face, or zero reference station. Figures 23, 24, 25, 26, and 29 present these data for the range of D/t ratios that were tested with one bearing position (position C). Figures 27 through 32 present these data for tests with all bearing positions for one D/t ratio (O.D. = 3.650 in.). These curves were plotted to obtain the general trend of the ovalization as the bearing face was approached and to permit the extrapolation of the curves up to the bearing face. The curves were extended with the assumption of a pseudo-bearing, one that was somewhat elastic and not as rigid as actual, on the basis that the ovalization would continue along the same trend if the clearance between the tube and the bearing remained constant.

Tests were conducted using compression loads in combination with bending loads and with compression loads only; these compression loads were applied eccentrically as well as in straight compression. No noticeable change in ovalization occurred when the compression loads were applied, even though the additional bending moment caused by the eccentric compression load would seem to indicate that the ovalization should increase. The maximum compression load used was 11,500 lbs. with a bending load of 6,000 lbs. These tests were made on the two tubes having the smallest thickness of wall. Inasmuch as it is shown that compression loads in combination with bending loads had little or no effect on the ovalization resulting from the bending load only, further tests with compression loads were not undertaken.

Some tests were also made on the various tubes with the bearing sleeve removed. The bearing sleeve referred to in this case is the bearing in the movable bearing. The bearing sleeve was removed and the movable bearing

base was raised so that the tube was supported in its original position. While the tests were not too closely related, the results showed that the slope of the ovalization vs. bending moment curve was definitely higher without the sleeve in place than with it. This higher slope can be interpreted to mean that the ovalization of the tube for a given load will increase as the clearance between the tube and the bearing sleeve is increased, although the magnitude of this increase has not been determined. As this effect was not considered until the investigation was more than half completed, sufficient data on the actual bearing clearances were not obtained and this effect could not be included in the final equation.

The ovalization was a maximum for a given bending moment at bearing position A, decreasing as the movable bearing was moved through positions B, C, and E. At bearing position D, however, the ovalization approaches that of position C, the reason for this being attributed to the change in the ratio of the distance between the opposite bearing faces and the outside diameter. This reasoning is based on the assumption that the portion of the tube between the two bearings reacts as a unit with the two bearings (the same effect as if the two bearings were rigidly tied together) until the movable bearing is placed beyond position C. As the movable bearing is moved toward position D, the fixed bearing end of the tube reacts as a restrained beam, but at the movable bearing the effect changes from a fully restrained to a partially restrained condition, the movable bearing tending to rotate somewhat with the tube as the load is applied, relieving some of the actual load on the tube at station zero.

The results indicate that the ovalization of a tube increases rapidly with the ratio of the distance between opposite bearing faces and the D/t ratio. The ovalization is dependent, however, not only on this ratio, but also on the bending moment and on the cantilever length of the tube.

DEVELOPMENT OF OVALIZATION FORMULA FOR MAXIMUM POSITIVE OVALIZATION AT STATION ZERO, 90° AZIMUTH

On log-log curve sheets (figs. 33 through 37) were

plotted the data for Ovalization vs. Bending Moment that were extrapolated to the zero reference station for the tubes with different ratios of D/t. The straight line trend of the points so obtained for any one given bearing position and D/t indicated the following relationship, which is merely the equation for the straight line on the log-log plot:

$$w = \frac{a\,M^{b}}{10^{4}}$$

or

$$\log w = \log a + b \log M - 4.0$$

where

w maximum positive ovalization at station zero, 90° azimuth, inches

M cantilever bending moment, inch-pounds

b slope of the line on the log-log plot

a constant for any one curve

and

10^{4} conversion from ten-thousandths of an inch to inches

Equations were then written for the curves of w vs. M for each bearing position and each D/t. The results indicated that the b terms (or slopes) were substantially constant for the curves for a fixed D/t, but that the a terms varied both with bearing position and D/t. It was necessary to make the a term of the general equation a function of both D/t and a value which depended upon the bearing position. The ratio of J to D/t was therefore used, where J is the distance in inches between outside bearing faces.

No direct relationship was found for the variation of the particular a terms with the ratio of J to D/t, but a plot of log (- log a) vs. the ratio J to D/t, as shown in figure 38, indicated a straight line variation for each bearing position with the curves for the five different bearing positions intersecting at a common point. Equations were deduced for each of these curves using the form:

$$\log (-\log a) = 0.10 + s \frac{J}{D/t}$$

or

$$\log a = -10^{\left(0.10+s\frac{J}{D/t}\right)}$$

where 0.10 is the Y-axis intercept of the five curves and s is the variable dependent upon bearing position.

No direct relationship was found between s and the cantilever length, L, but a plot of log [log (10 s)] vs. log (log L) resulted in a straight line variation (as shown in fig. 39) for which the following equation was written:

$$\log [\log (10\ s)] = -3.465 + 14.1920 \log (\log L)$$

or

$$\log (10\ s) = 0.000343\ (\log L)^{14.1920}$$

where L is the cantilever length, in inches.

As stated on page 9, the trend of the b terms (or slope of the log-log plot of w vs. M, figs. 33 through 37) indicated that the slopes were substantially constant for a given D/t. Averaging the practically constant values of b for the sets of curves with constant D/t, values of b were obtained which were plotted against D/t in figure 41. The following empirical equation was deduced for the curve obtained:

$$b = \frac{\log (D/t) - 1.143}{3.06 - 5.90 \log (D/t)} + 0.75$$

It is to be noted here that the agreement of the curves drawn using these slopes with the log-log w vs. M data for some of the curves of D/t of 7.00 and 7.55 is not as good as for the data with the other D/t ratios. The data obtained for these two D/t ratios were obtained using the parallel arm gage as opposed to the double indicator gages used in obtaining the remainder of the data. In addition, the data for the D/t of 7.55 were obtained using a sleeve with a very large

clearance, hence the increased slope. It is thought, however, that the curve as shown in figure 41 of b vs. D/t gives within reasonable limits the slopes that would have been obtained had the data for these D/t ratios been taken under the same conditions as for the others.

A summary of the empirical equations deduced is as follows:

$$w = \frac{a\,M^{b}}{10^{4}} \qquad (1)$$

$$\log w = \log a + b \log M - 4.0 \qquad (2)$$

$$\log w = -10^{\left(0.10+s\frac{J}{D/t}\right)} + b \log M - 4.0 \qquad (3)$$

$$\log (10\,s) = 0.000343\,(\log L)^{14.1920} \qquad (4)$$

$$b = \frac{\log (D/t) - 1.143}{3.060 - 5.90 \log (D/t)} + 0.75 \qquad (5)$$

In order to facilitate the determination of s in any particular case, values were calculated using formula (4), giving s for a range of cantilever lengths, L, from 10 to 60 inches. Figure 40 contains the curve plotted from these values and it also shows the experimental points from which the equation was deduced.

For determination of b, equation (5) was solved to give values of b for values of D/t from 5 to 20. The results are plotted in figure 41.

The recommended procedure for determining ovalization when M, D/t, J, and L are known, is to determine s from figure 40, determine b from figure 41, substitute these values along with the other knowns in equation (3), and solve for w.

CONCLUSIONS

1. Tubes of the type commonly used in landing gear struts were shown to ovalize to such an extent under normal operating loads that "freezing" of the strut will result if adequate clearance is not allowed in the bearing, or if means are not introduced to stiffen the tube sufficiently to prevent excessive ovalization.

2. The compression load, acting in straight compression or eccentrically, in combination with a bending load does not affect the ovalization. The eccentricity of the compression load in these tests did not exceed four inches and a greater eccentricity may not act in the same manner, as when the bending effect overrides the straight compression effect.

University of Notre Dame,
Notre Dame, Ind., January 10, 1944.

BIBLIOGRAPHY

1. Timoshenko, S.: Theory of Elasticity, 1934.

2. Vigness, Irwin: Elastic Properties of Curved Tubes, Transactions of the A.S.M.E., February 1943.

3. Davis, D. S.: Empirical Equations and Nomography, 1943.

4. Roark, R. J.: Formulas for Circular Rings, Product Engineering, July 1937.

5. Miller, Roy A., and Wood, Karl D.: Formulas for the Stress Analysis of Circular Rings in a Monocoque Fuselage. T.N. No. 462, NACA, 1933.

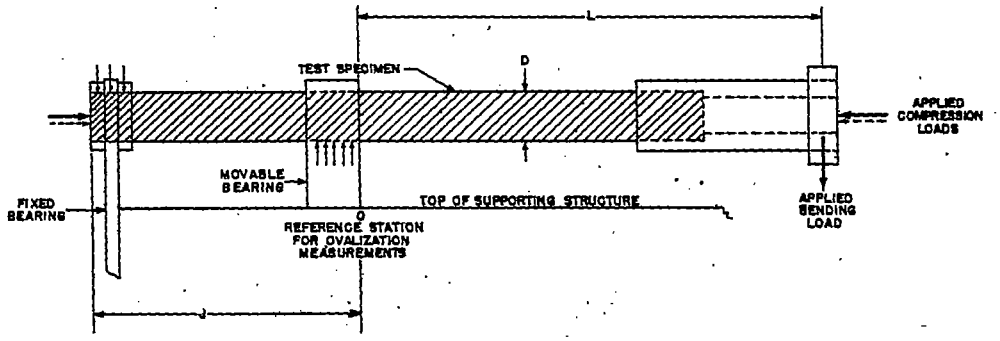

Figure 1.- Simplified sketch of the apparatus and method of testing.

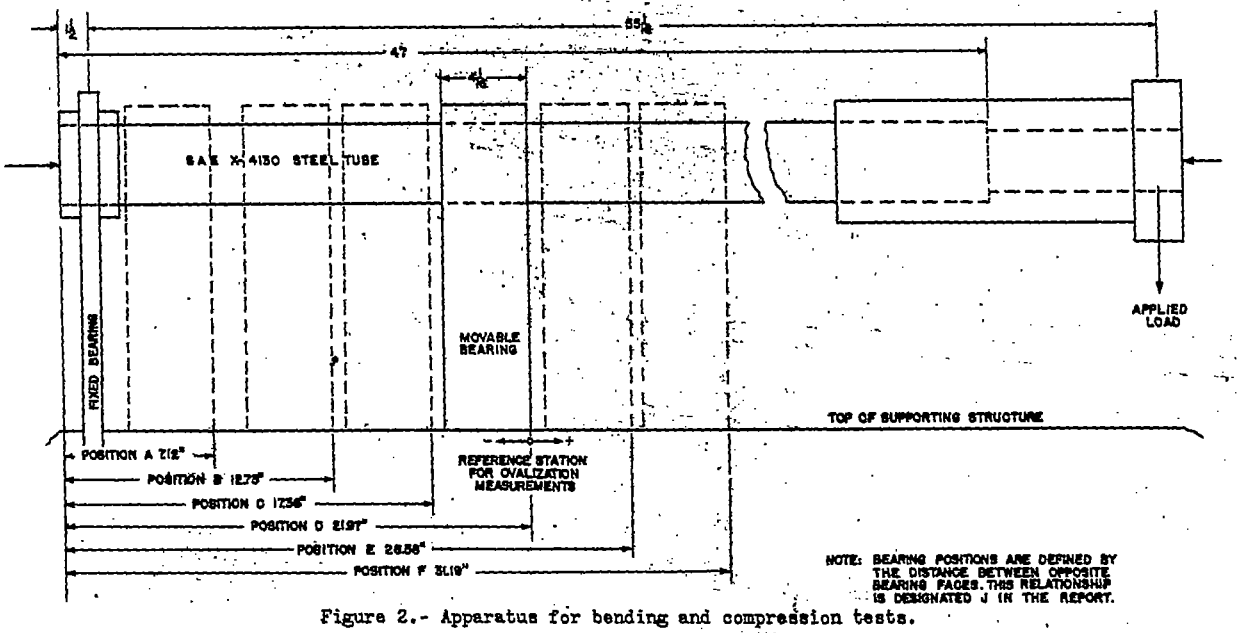

Figure 2.- Apparatus for bending and compression tests.

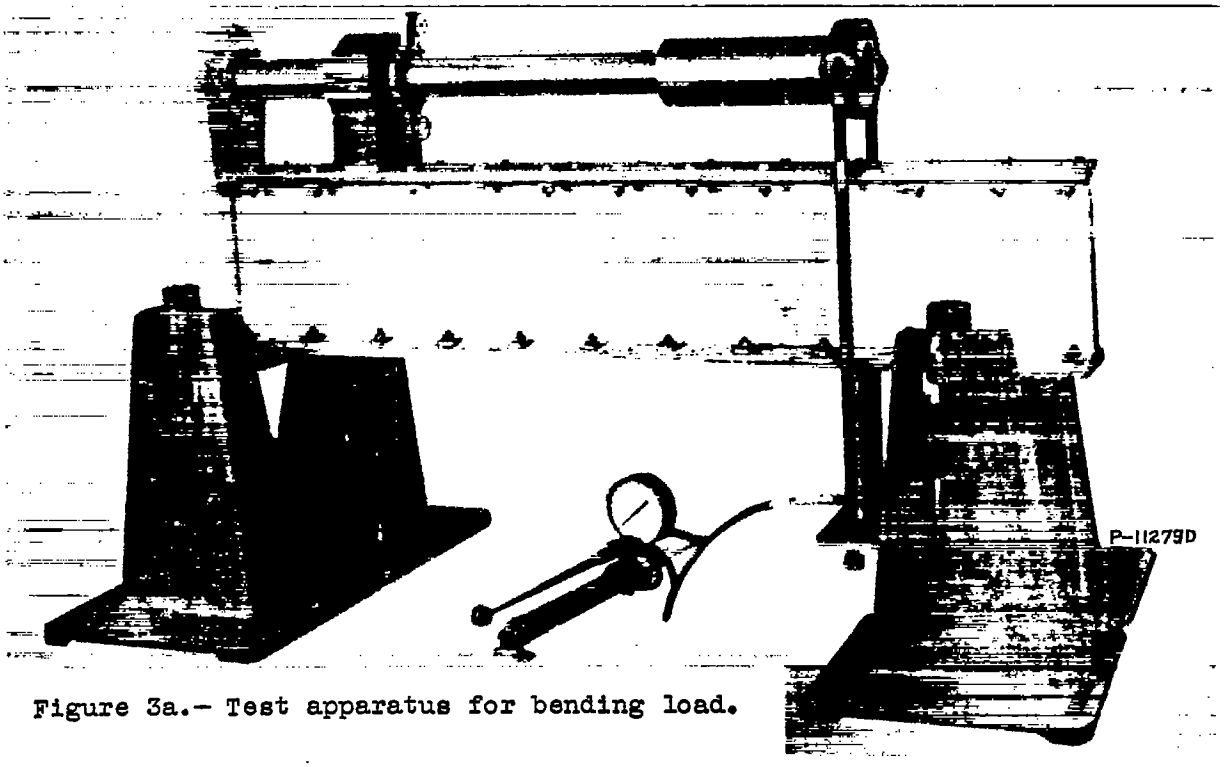

Figure 3a.- Test apparatus for bending load.

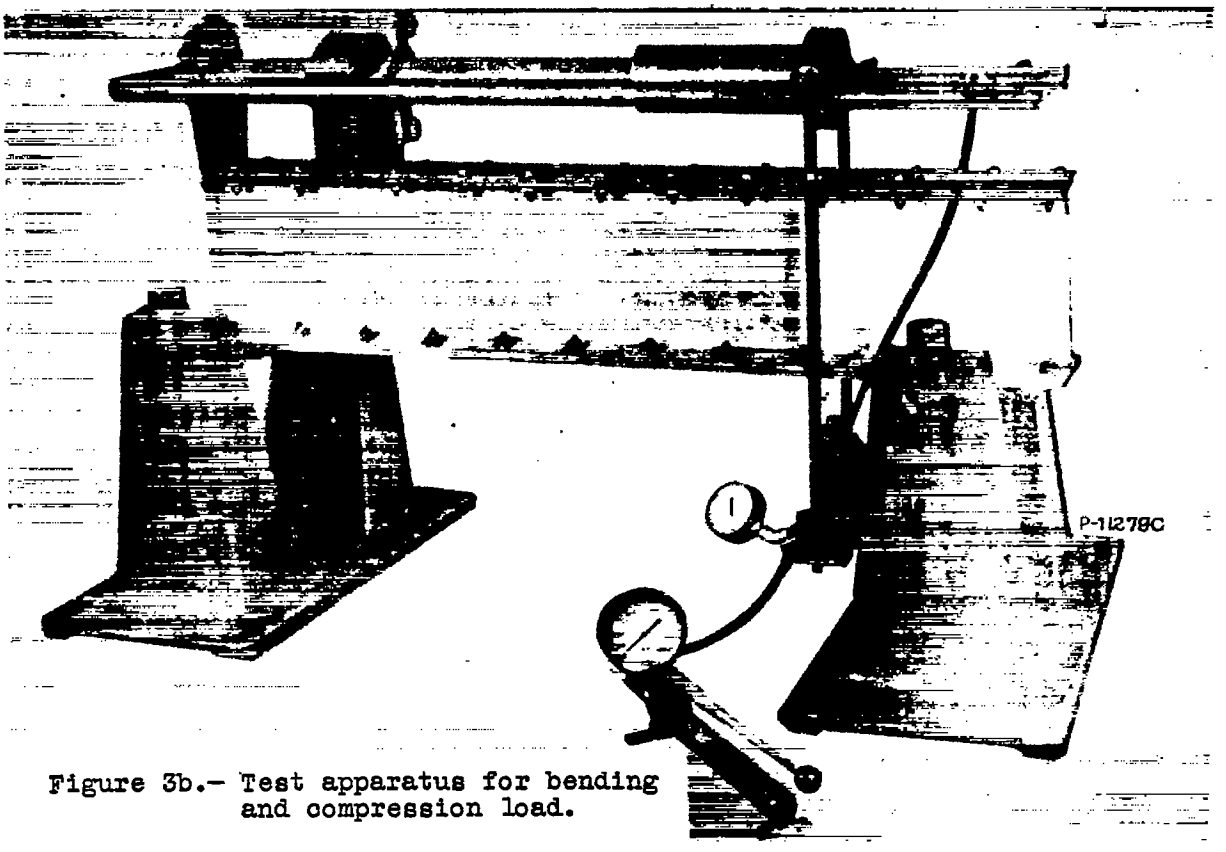

Figure 3b.- Test apparatus for bending and compression load.

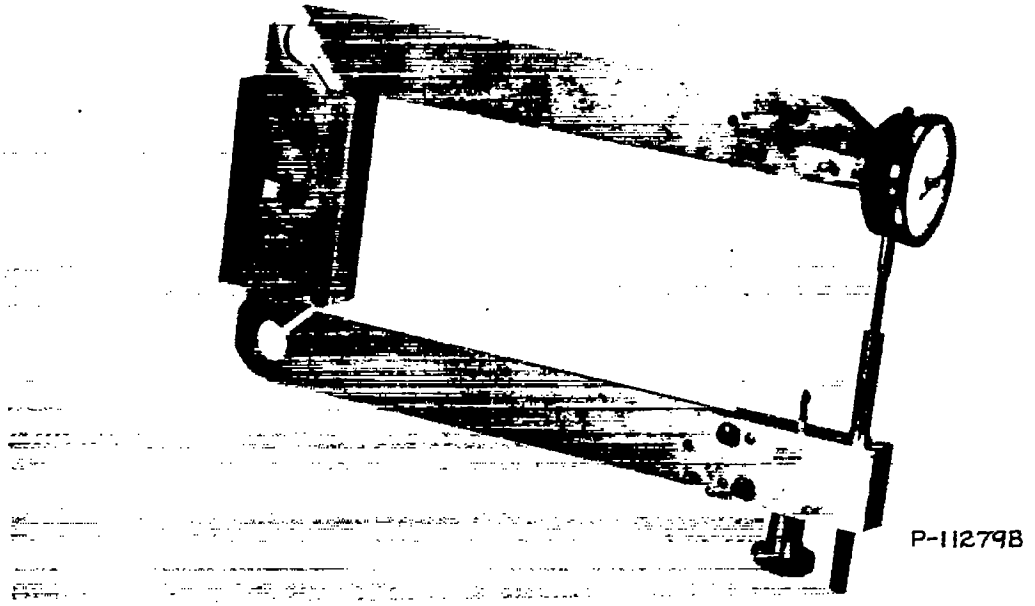

Figure 4.- Parallel-arm type ovalization gage.

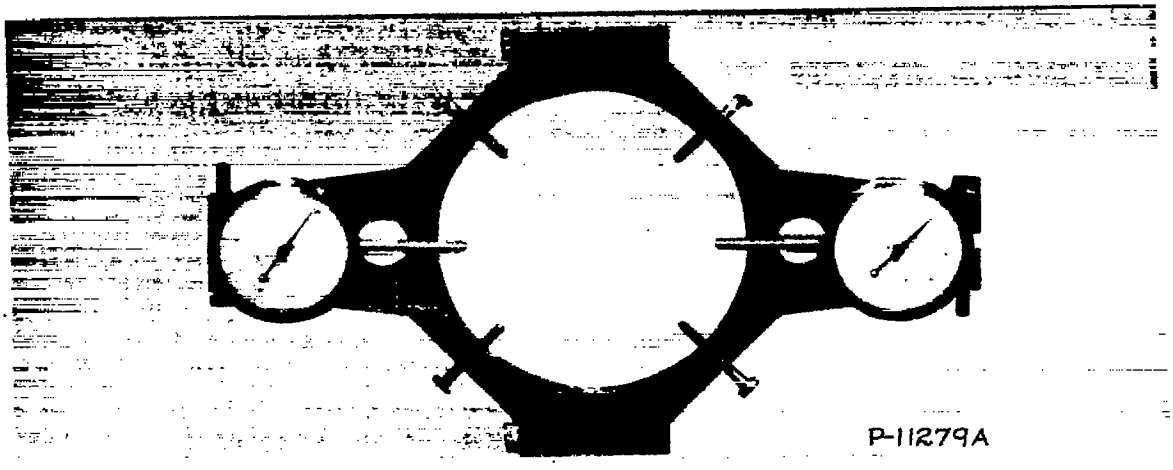

Figure 5.- Double-indicator type ovalization gage.

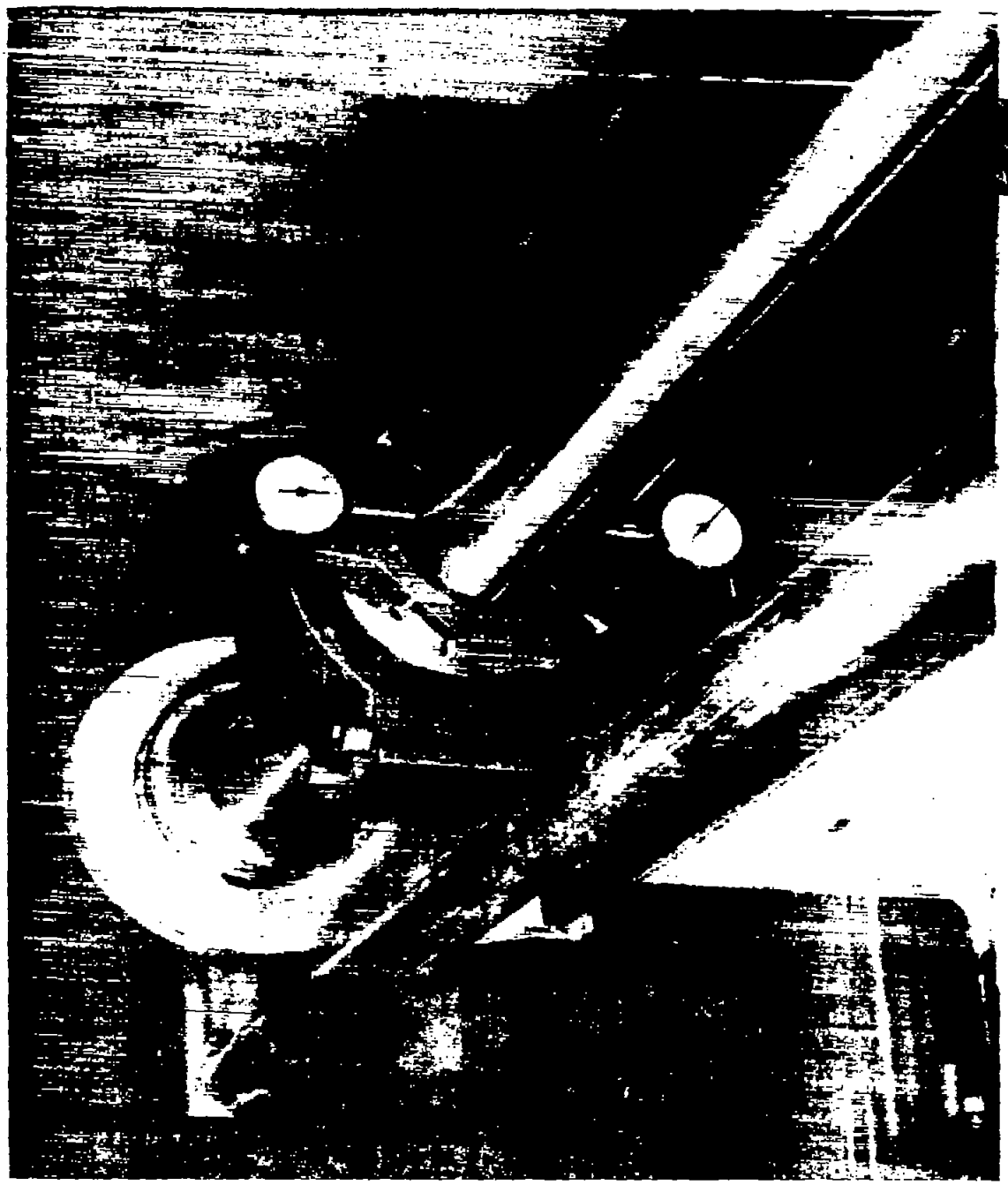

Figure 6.- Double-indicator type gage on tube at station 1.5

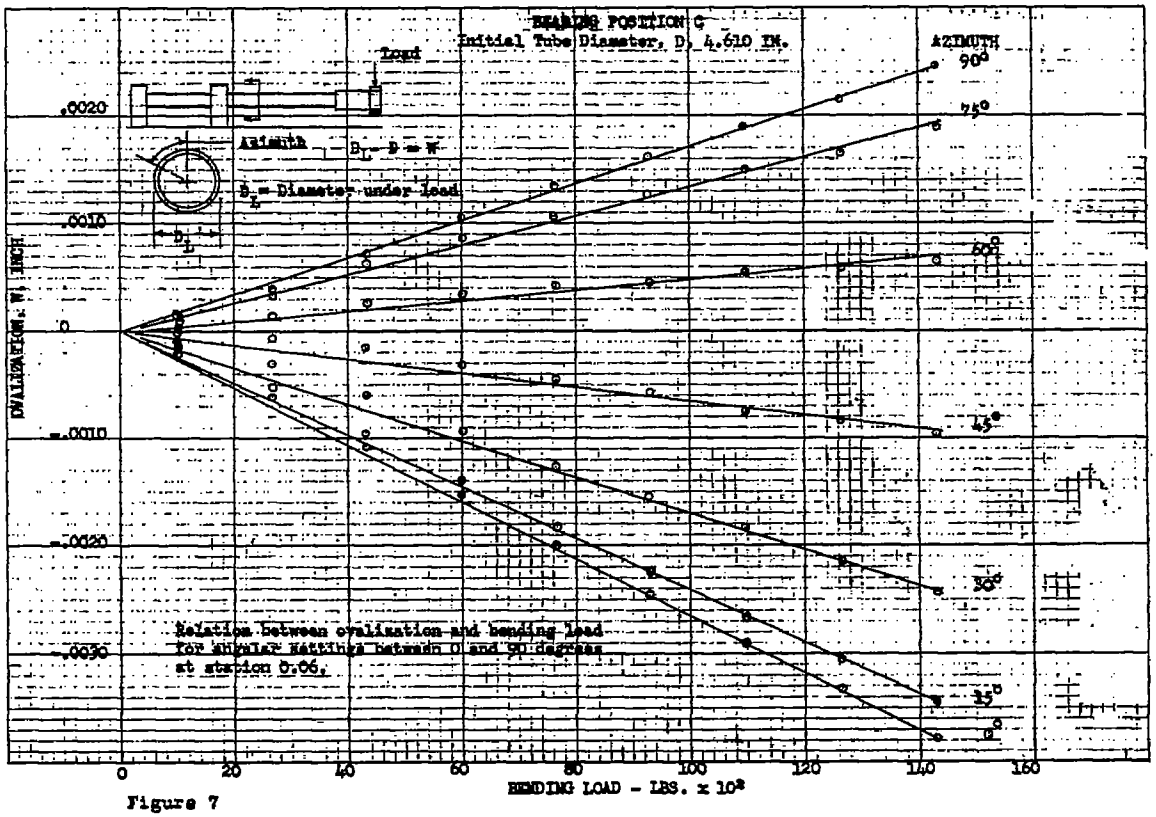

Figure 7

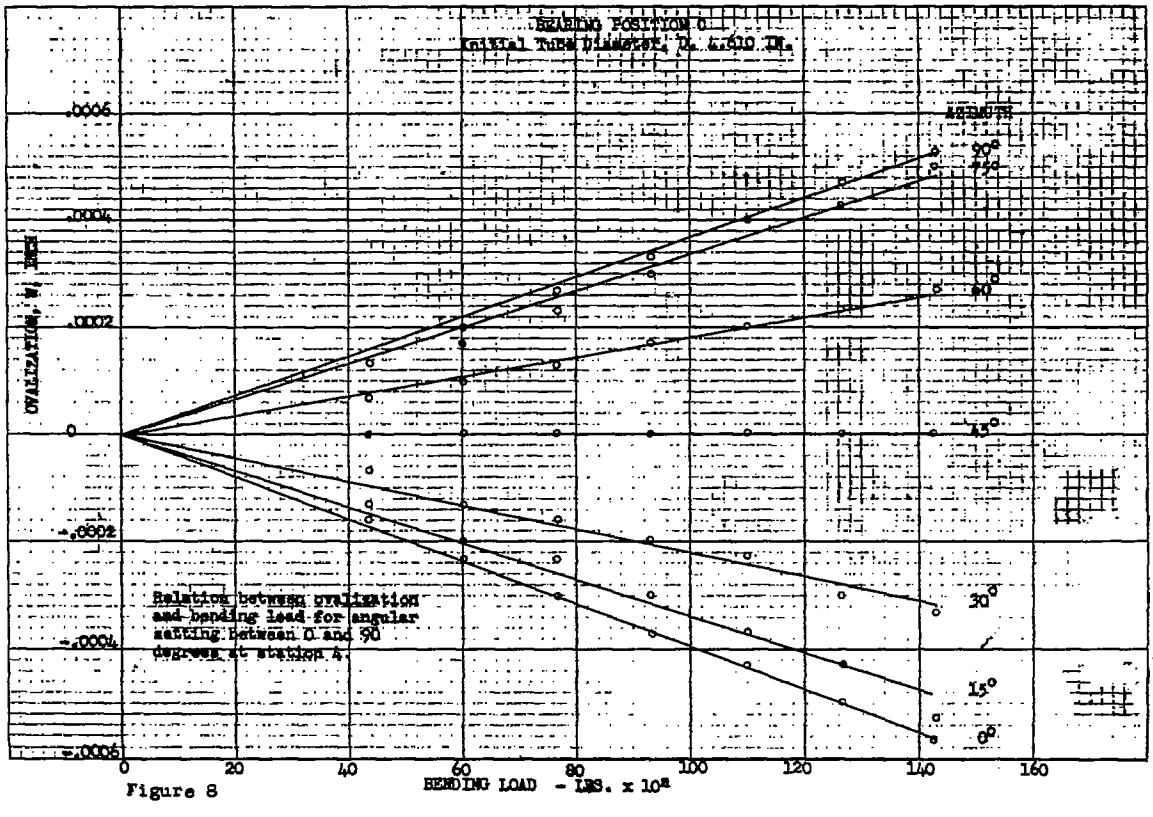

Figure 8

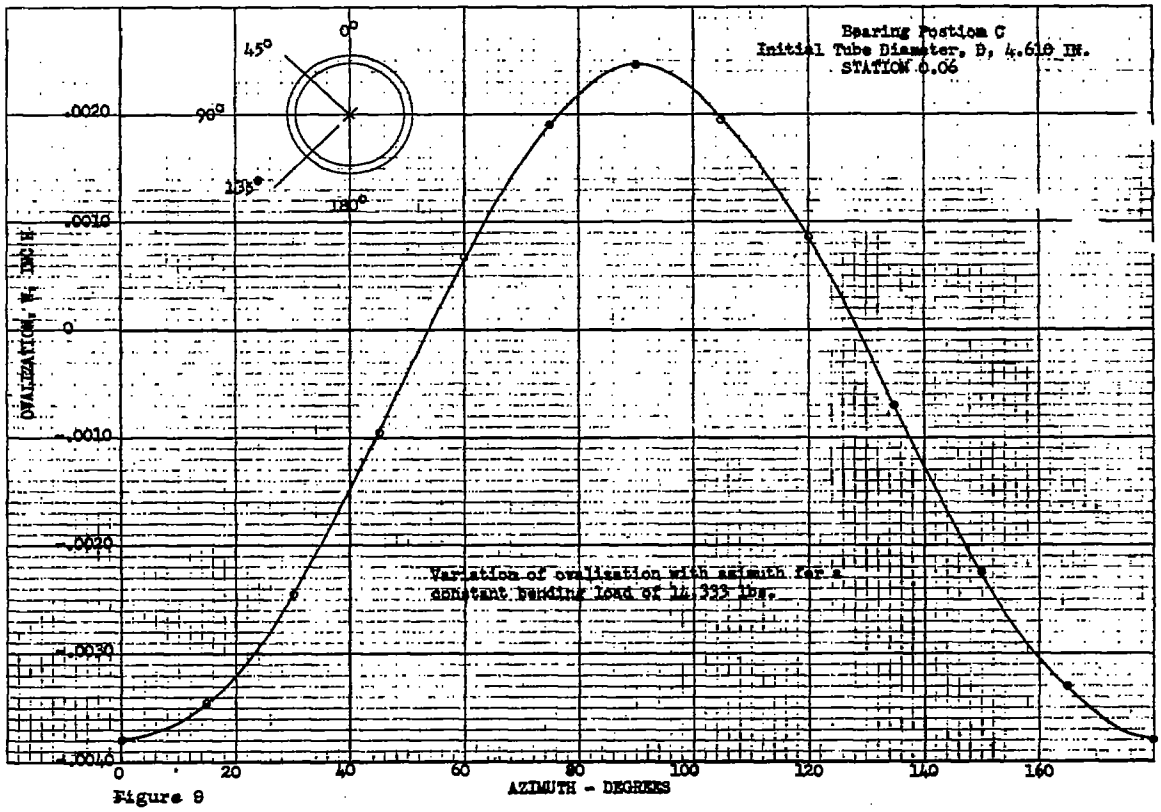

Figure 9

Variation of ovalization with azimuth for a constant bending load of 14,333 lbs.

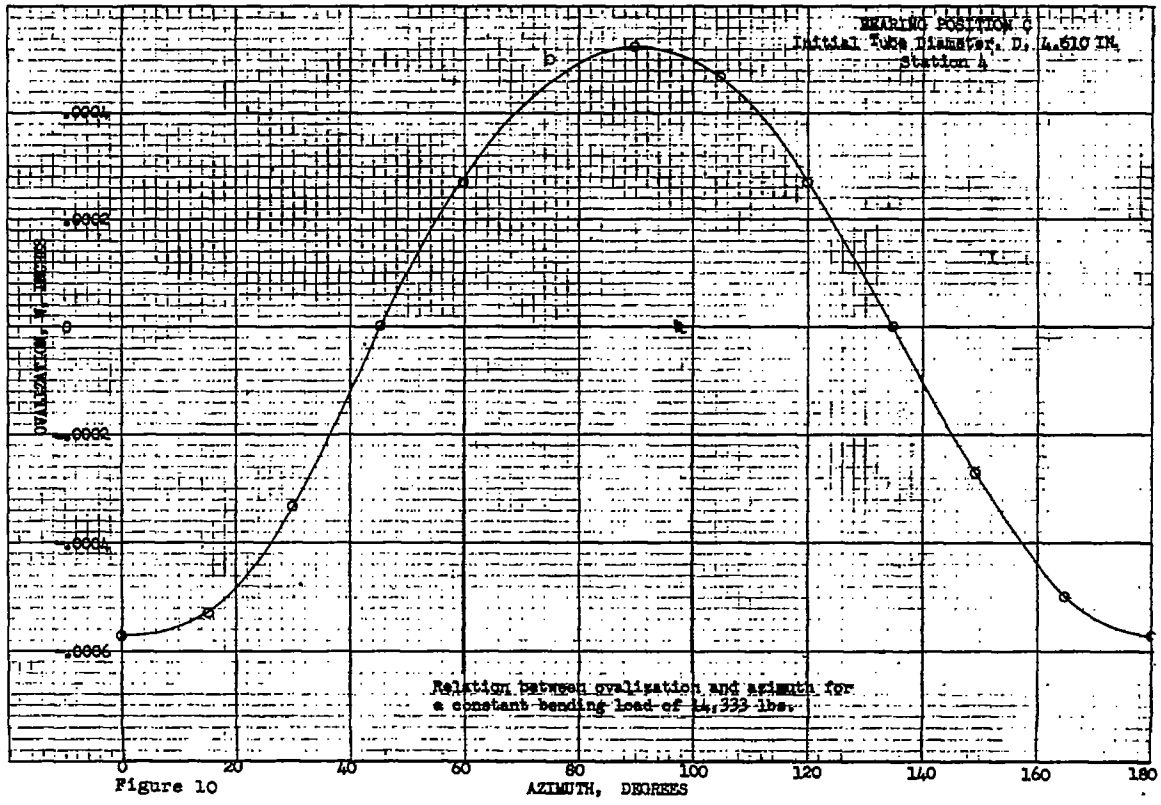

Figure 10

Relation between ovalization and azimuth for a constant bending load of 14,333 lbs.

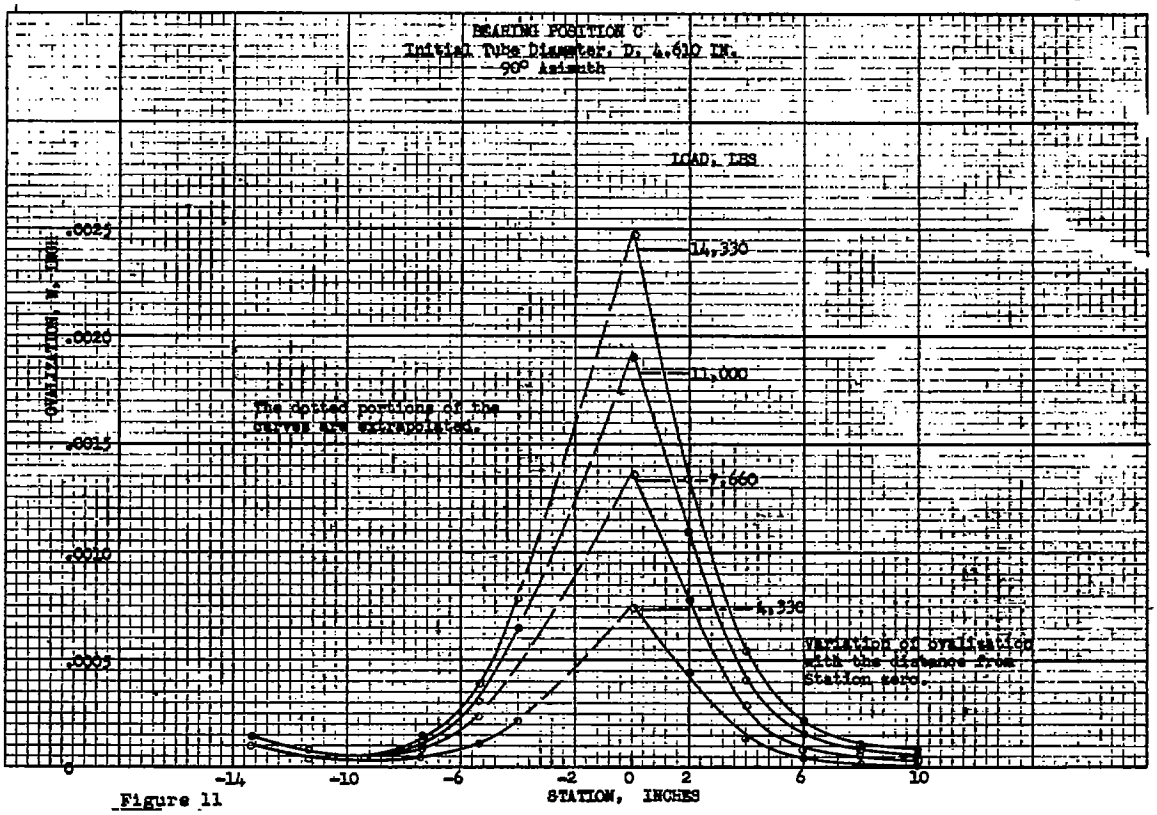

Figure 11

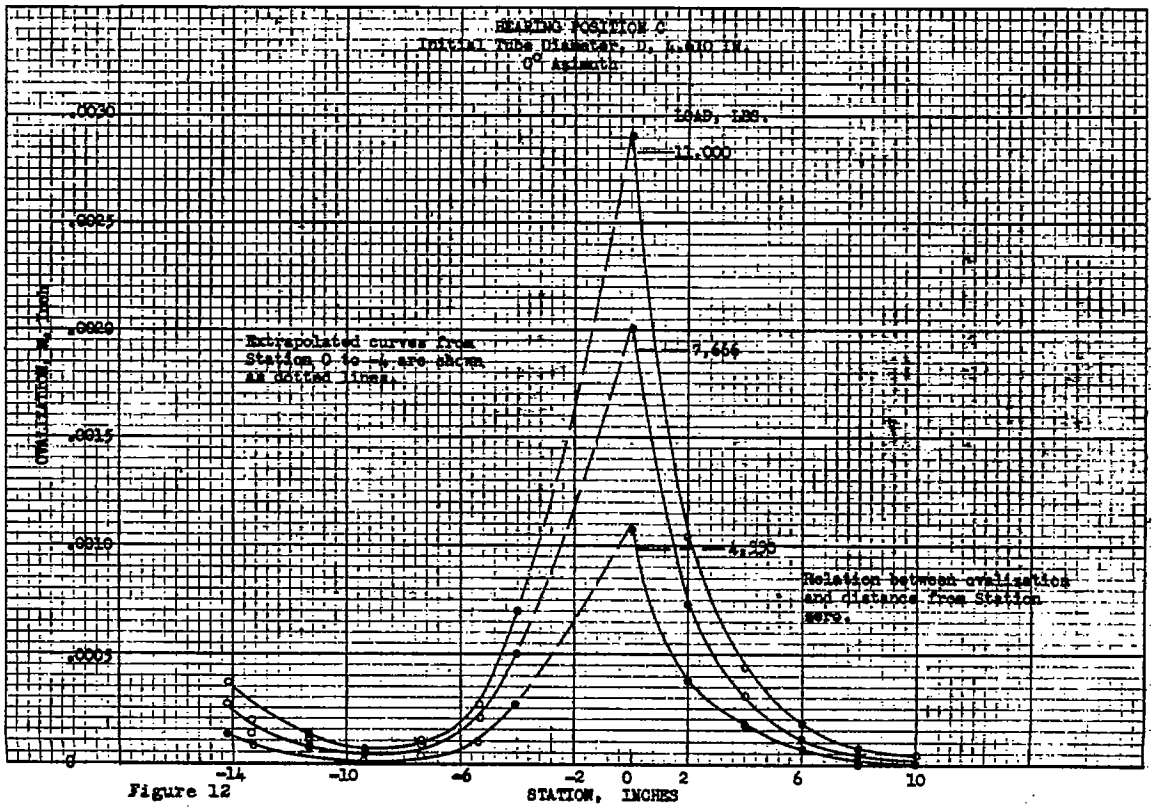

Figure 12

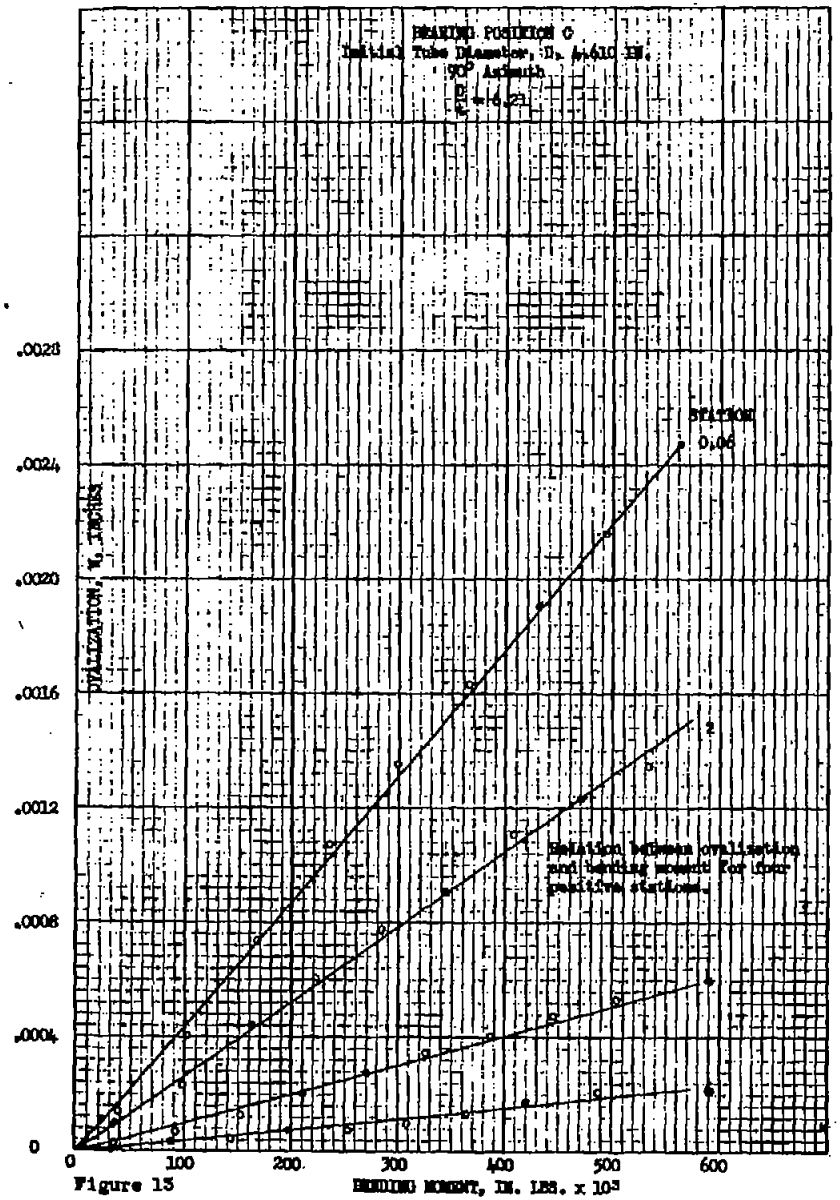

Figure 13

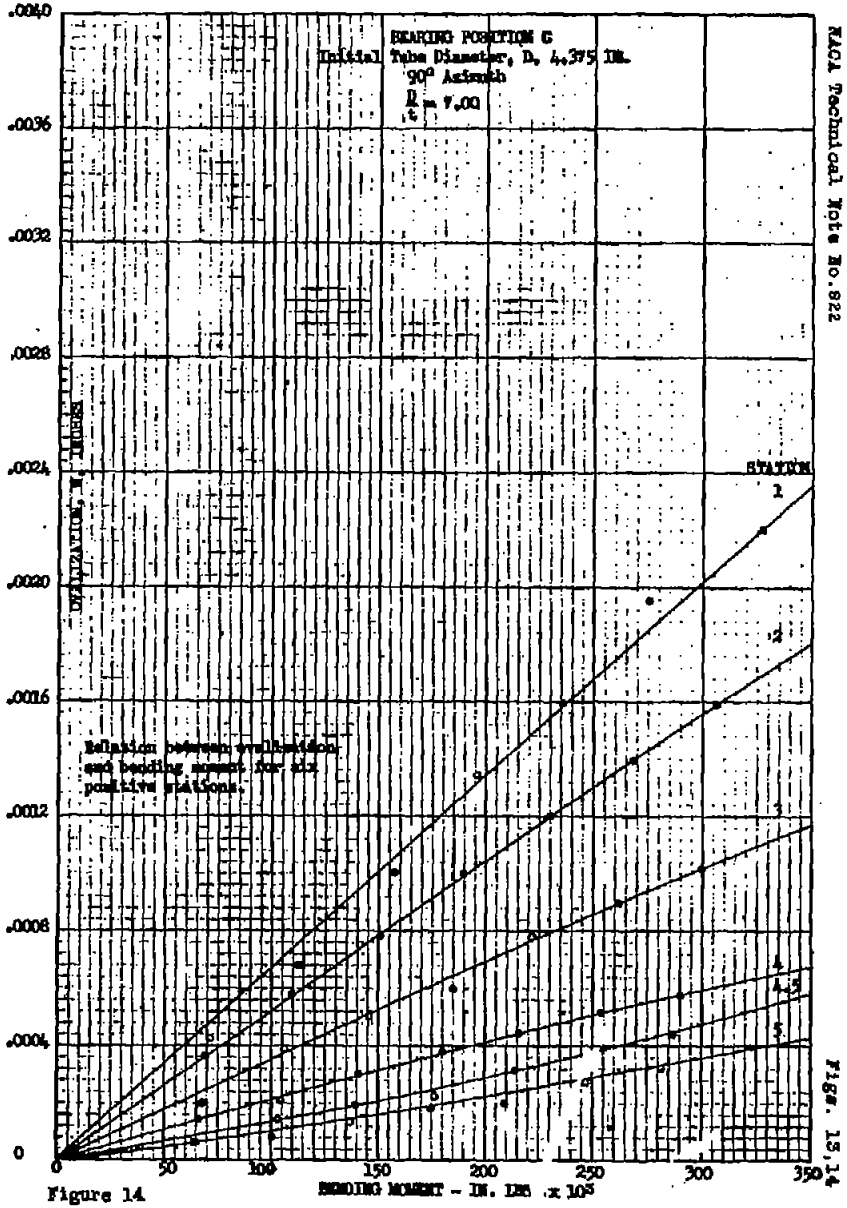

Figure 14

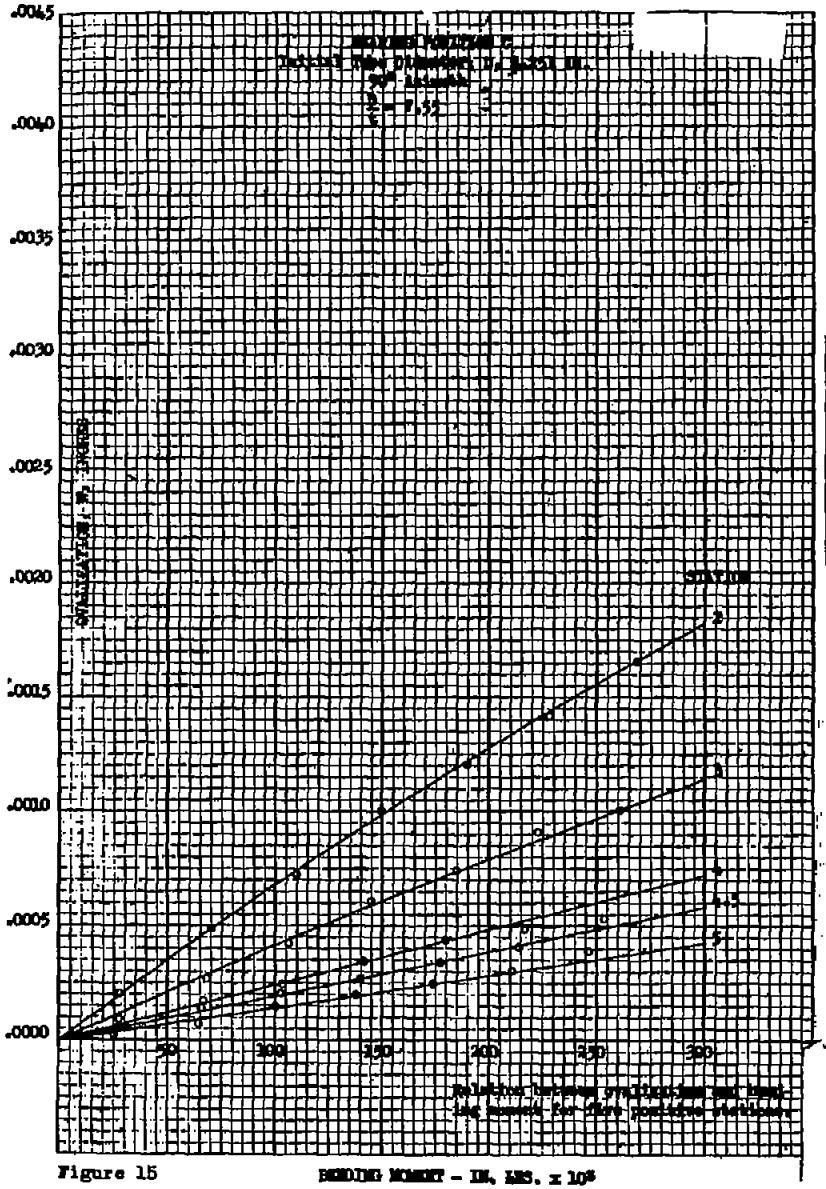

Figure 15

BENDING MOMENT - IN. LBS. x 10^3

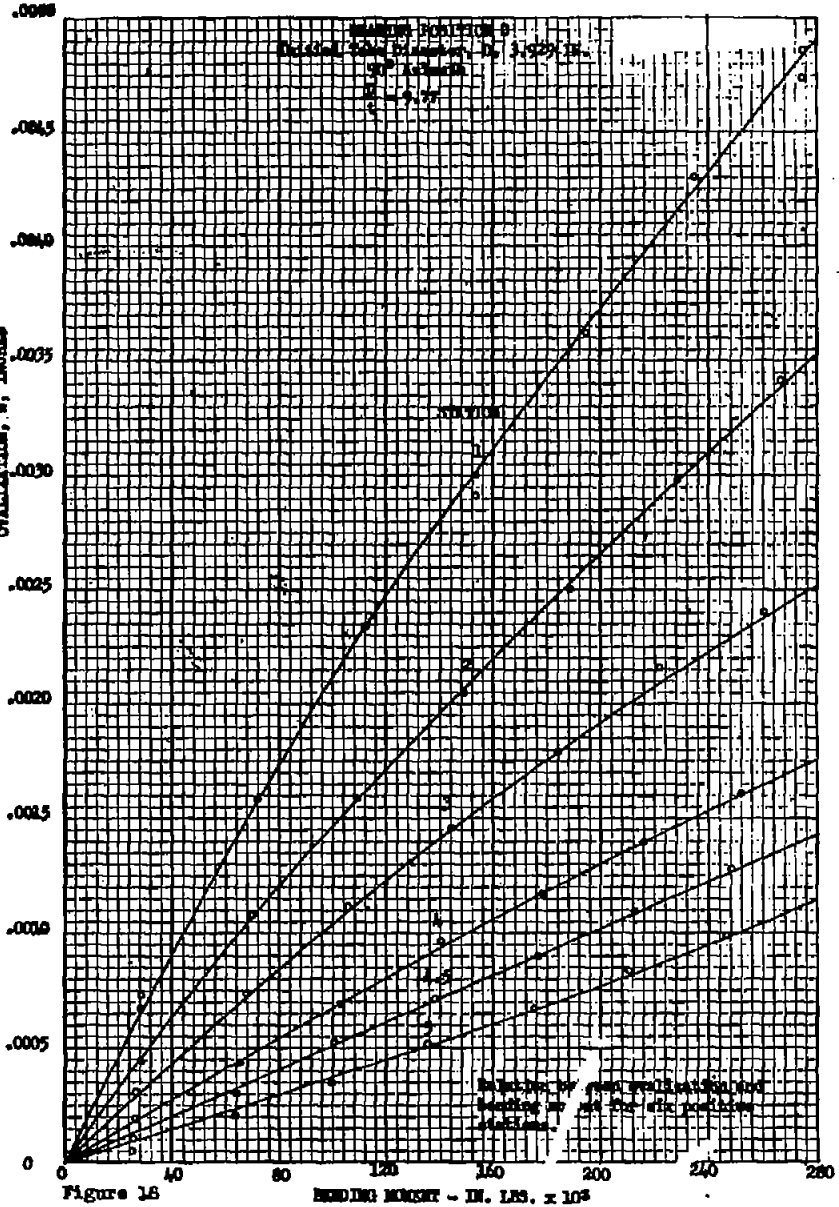

Figure 16

BENDING MOMENT - IN. LBS. x 10^3

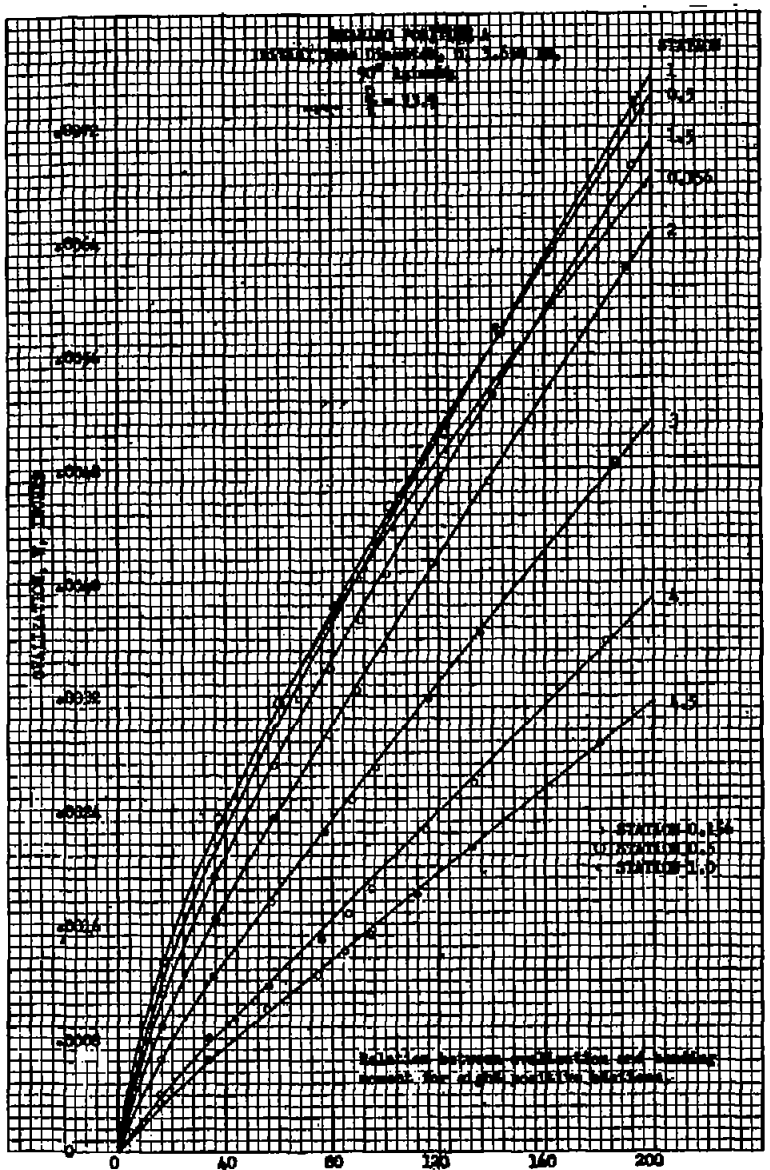

Figure 17

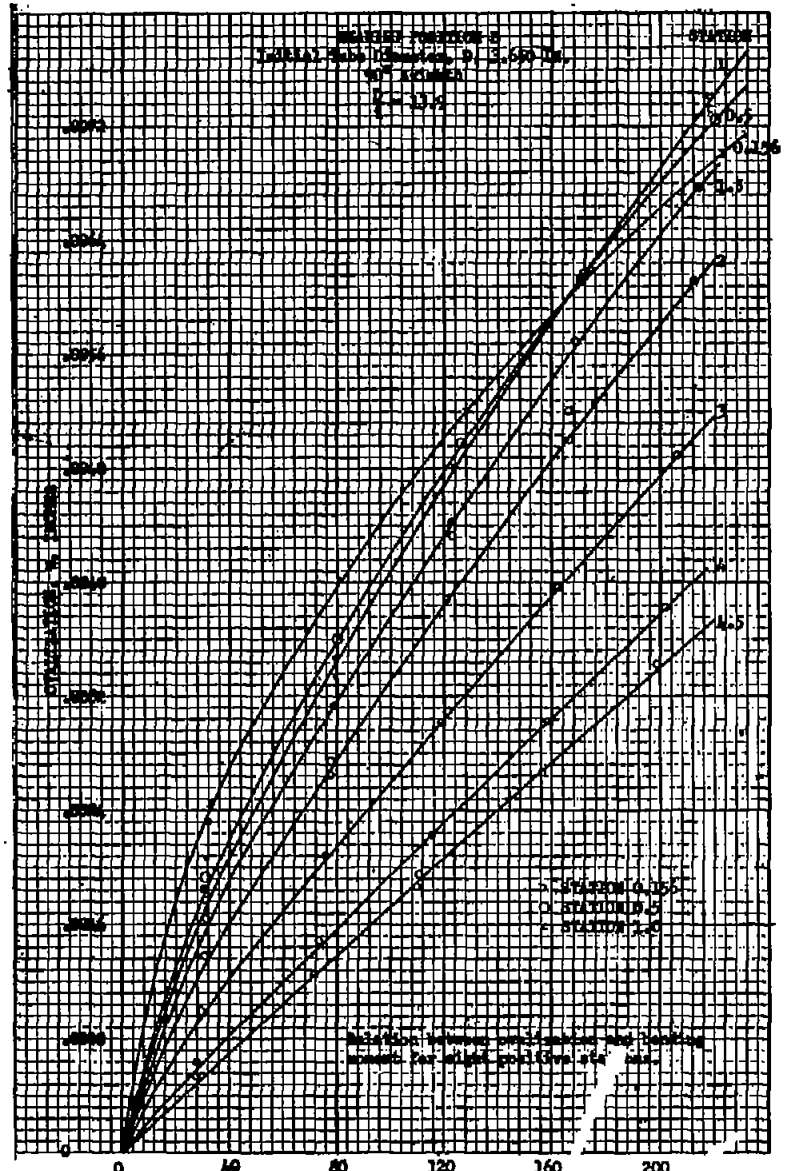

Figure 18

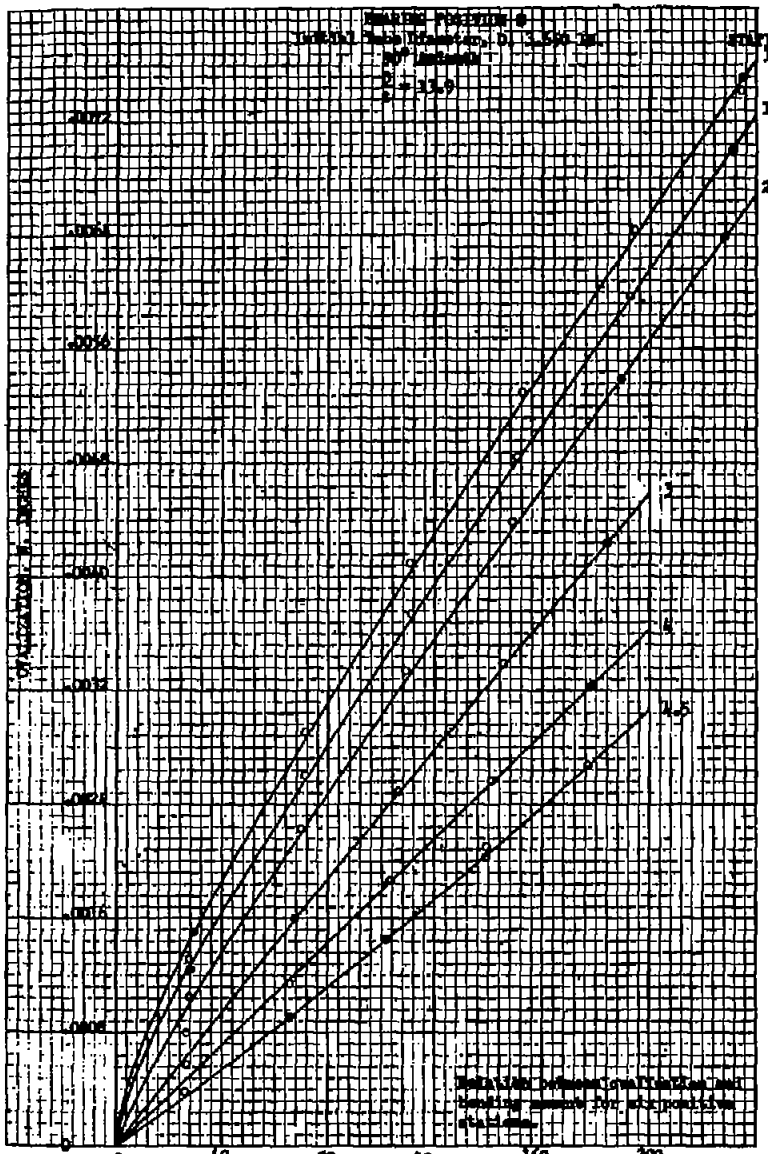

Figure 19 BENDING MOMENT - IN. LBS. x 10^3

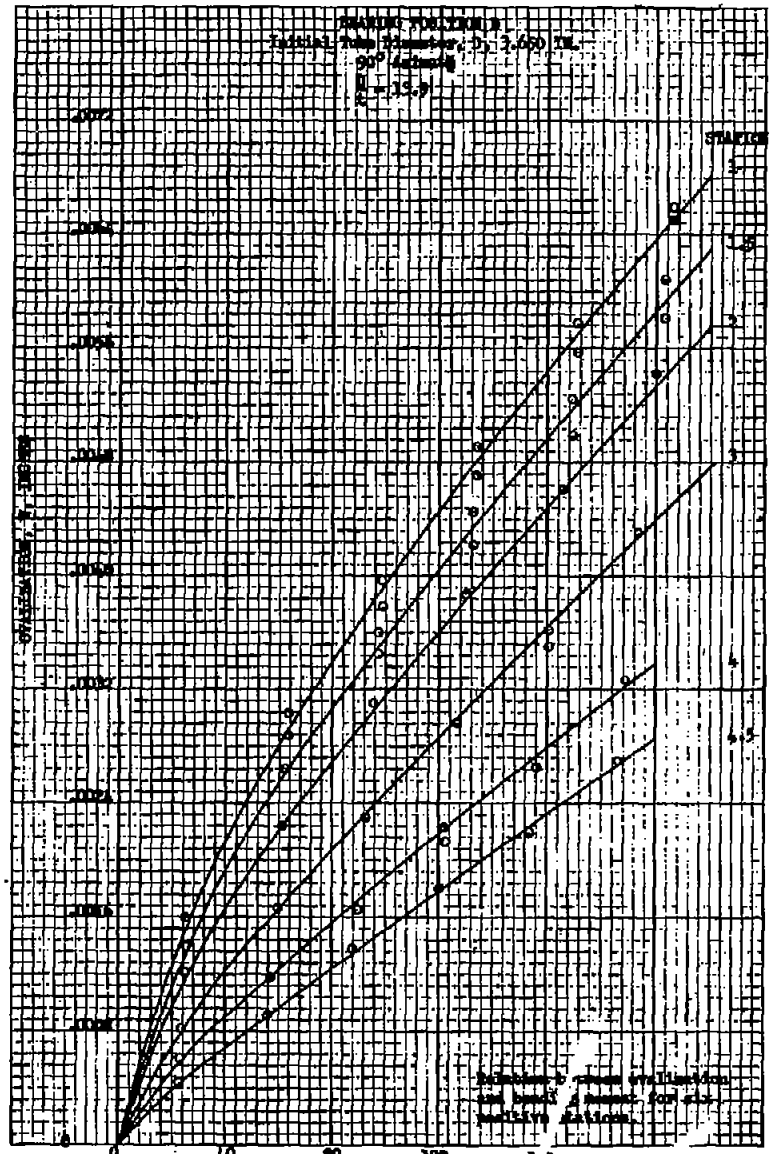

Figure 20 BENDING MOMENT - IN. LBS. x 10^3

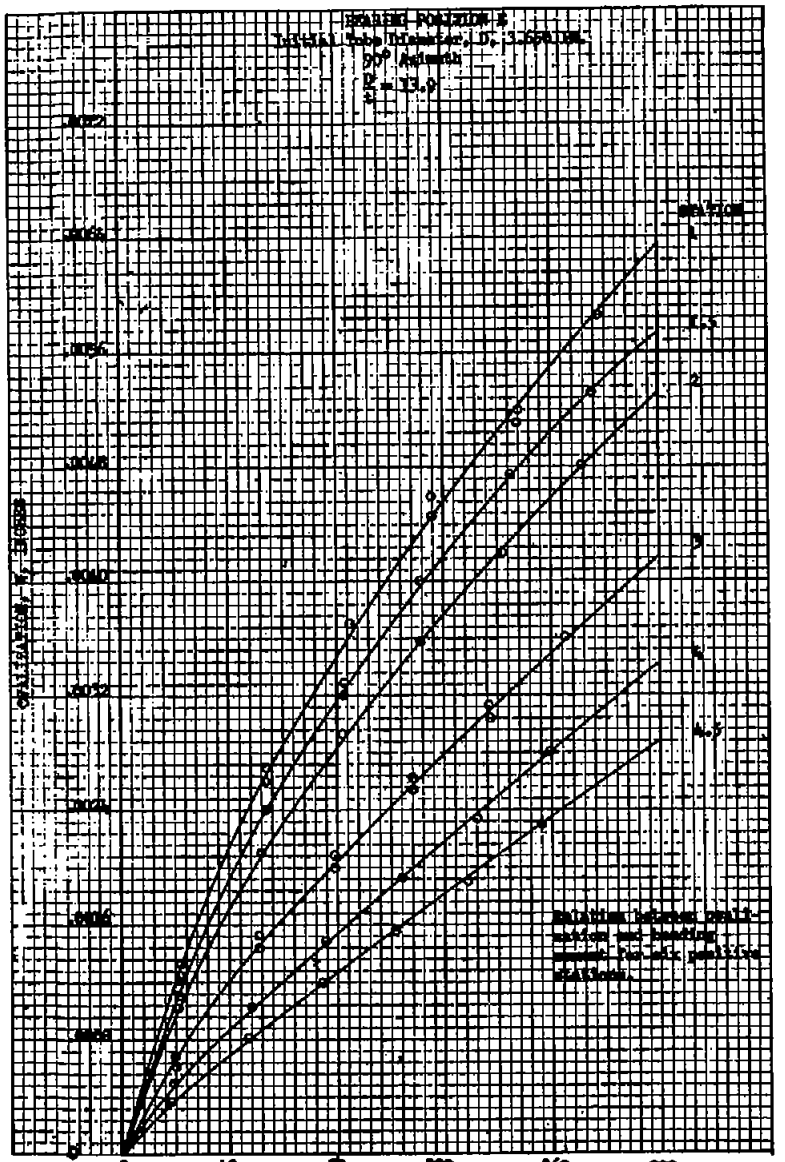

Figure 21

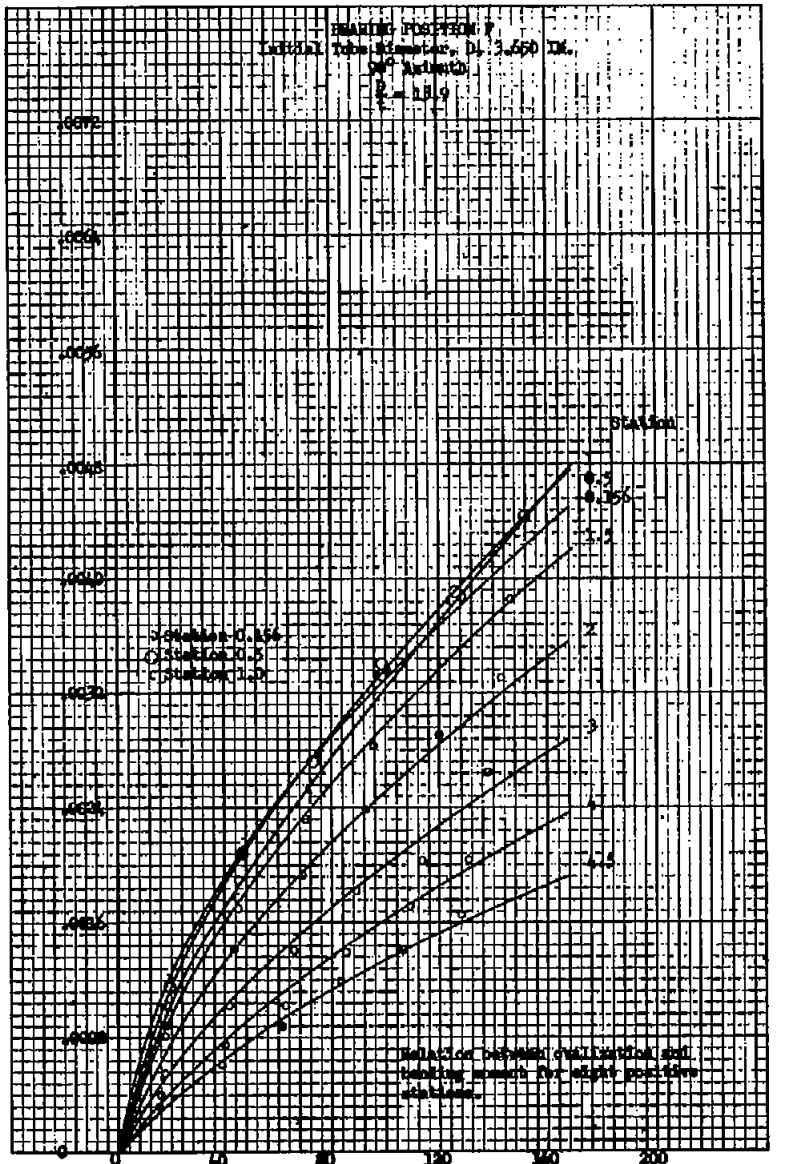

Figure 22

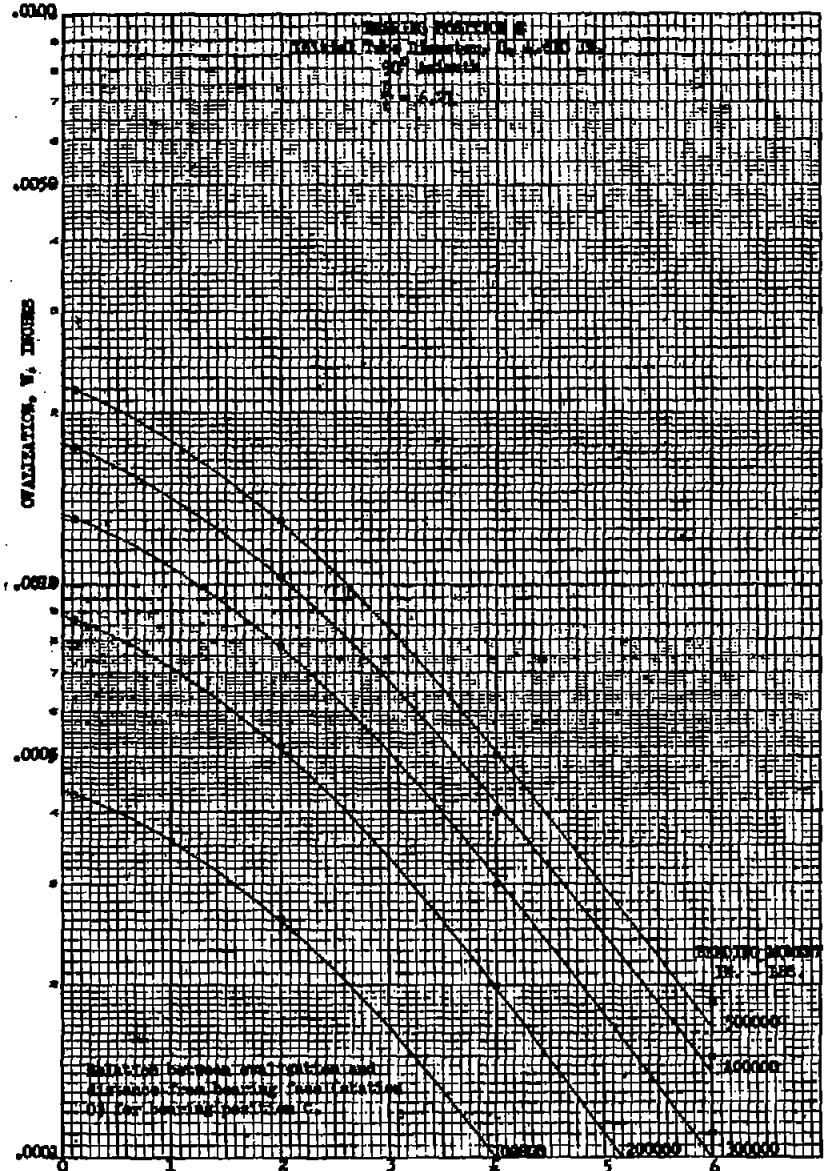

Figure 23

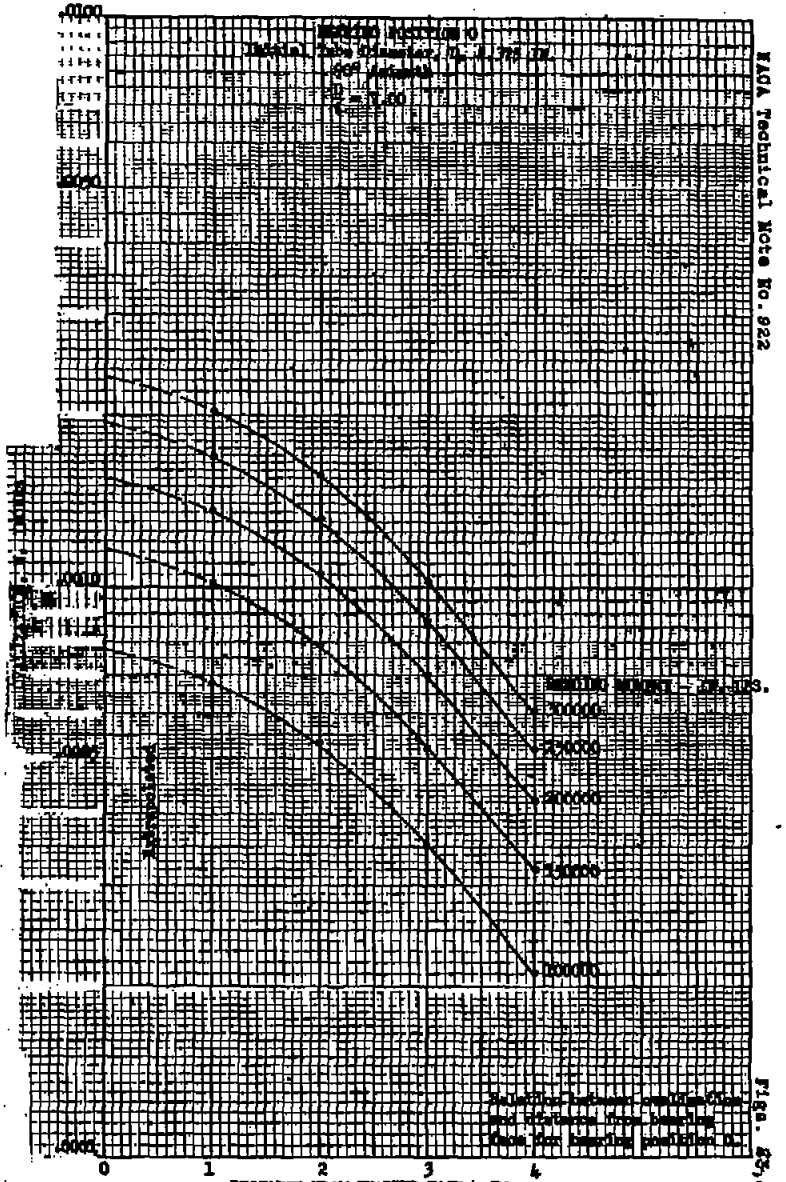

Figure 24

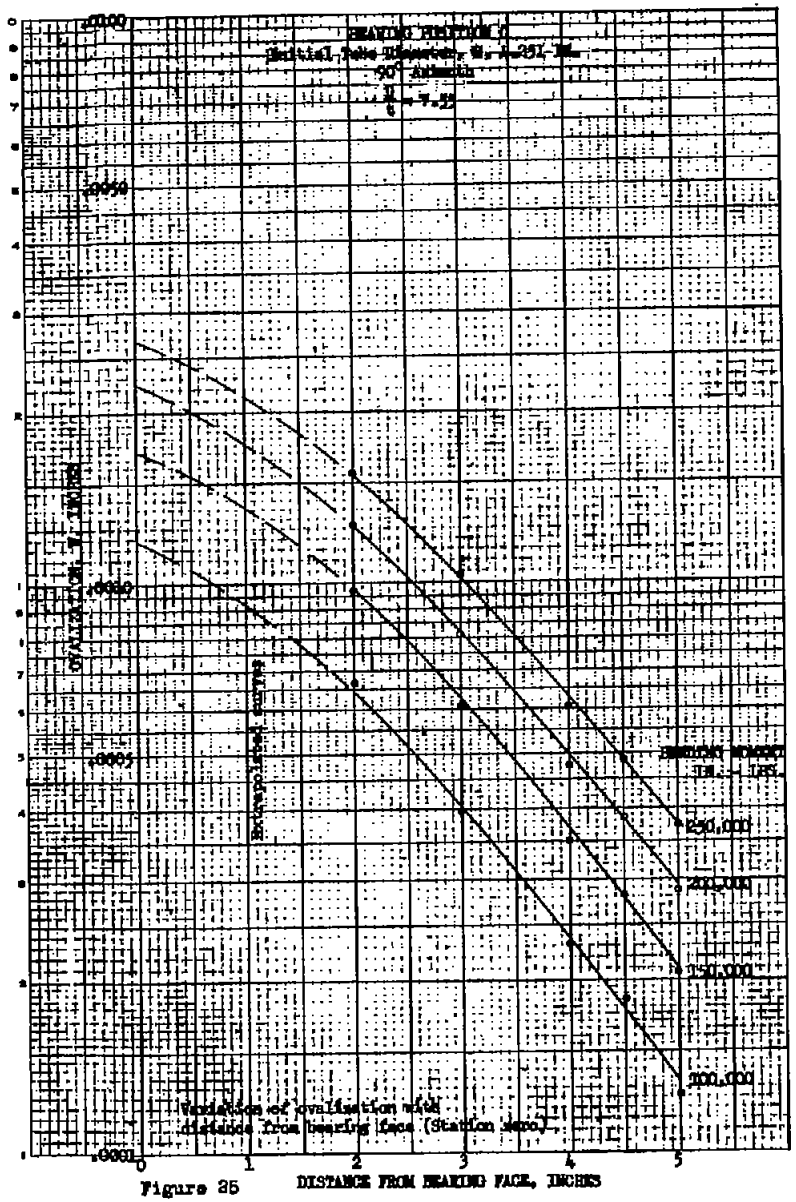

Figure 25

Variation of ovalization with distance from bearing face (Station zero).

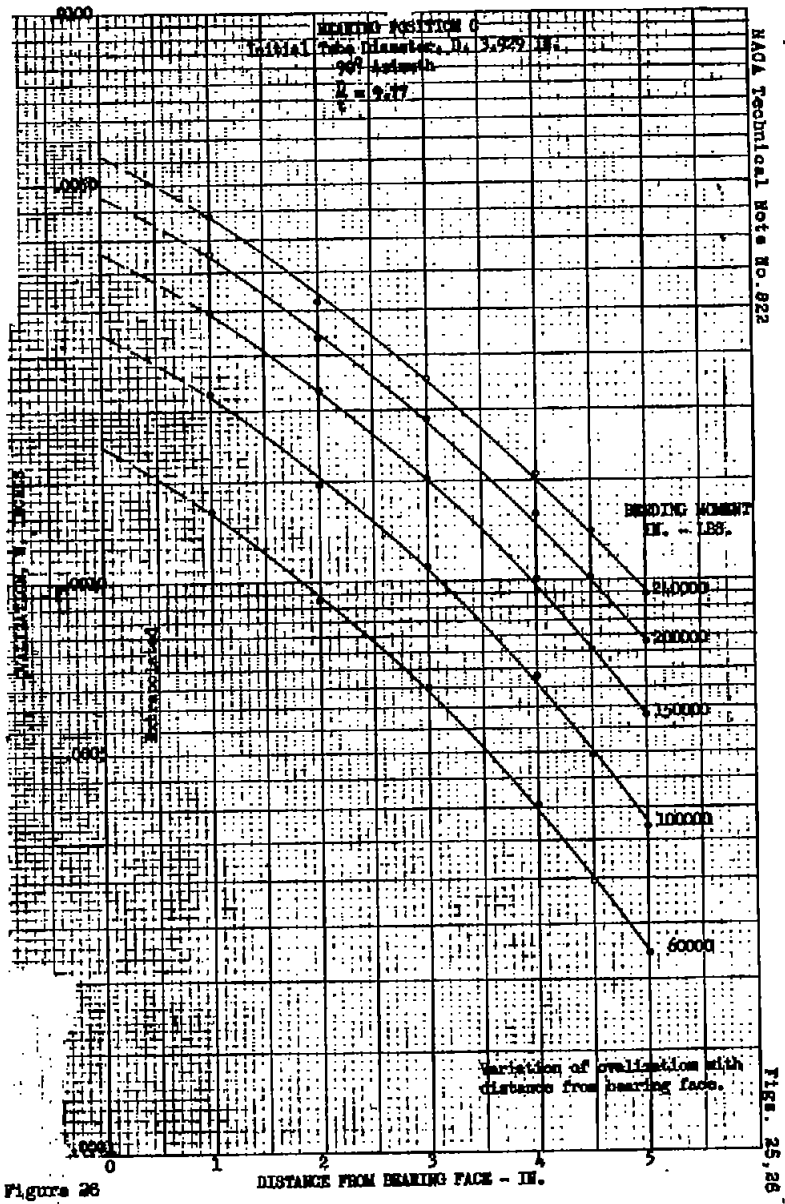

Figure 26

Variation of ovalization with distance from bearing face.

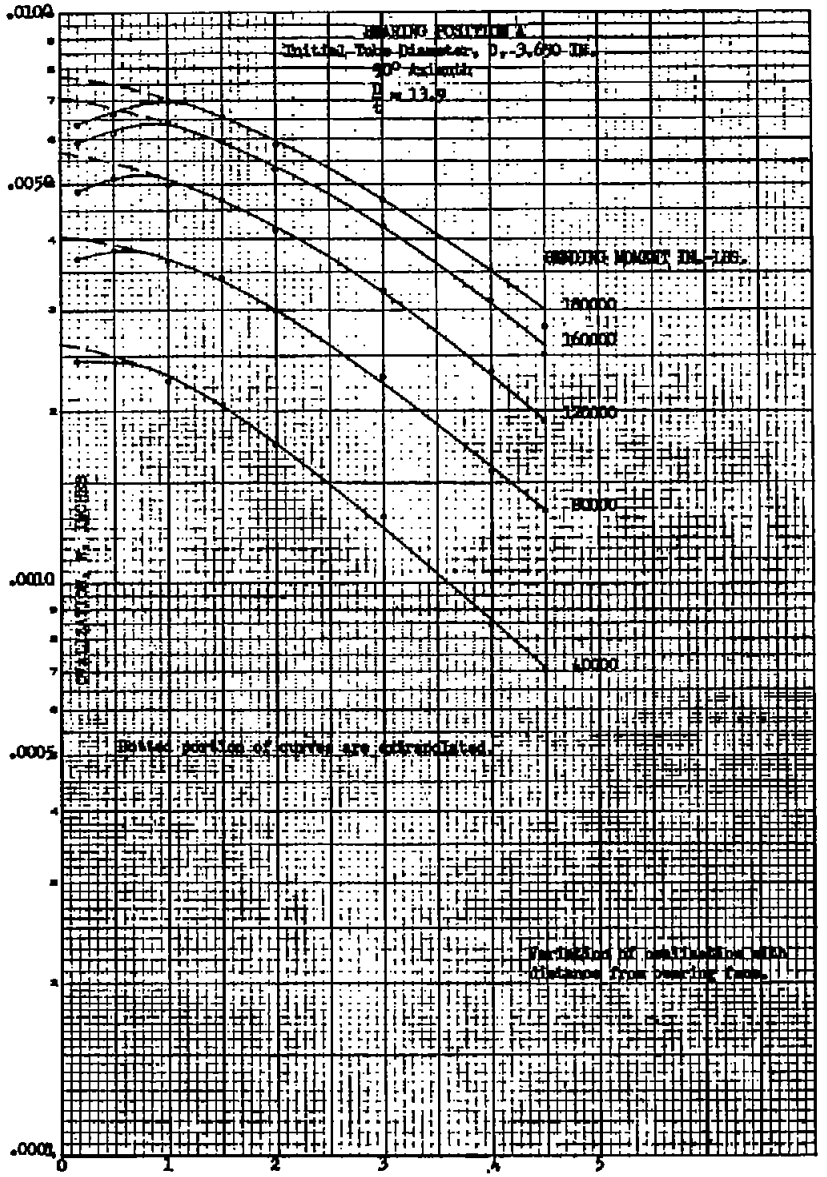

Figure 27

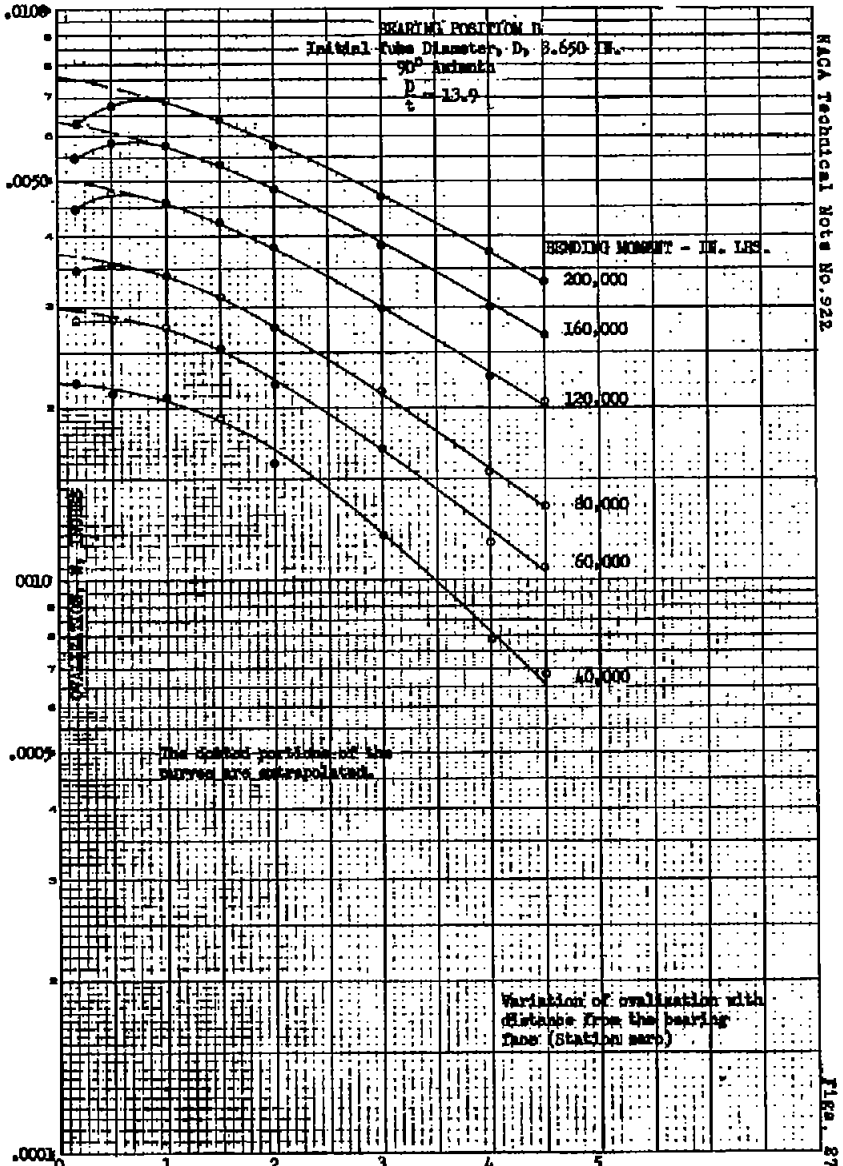

Figure 28

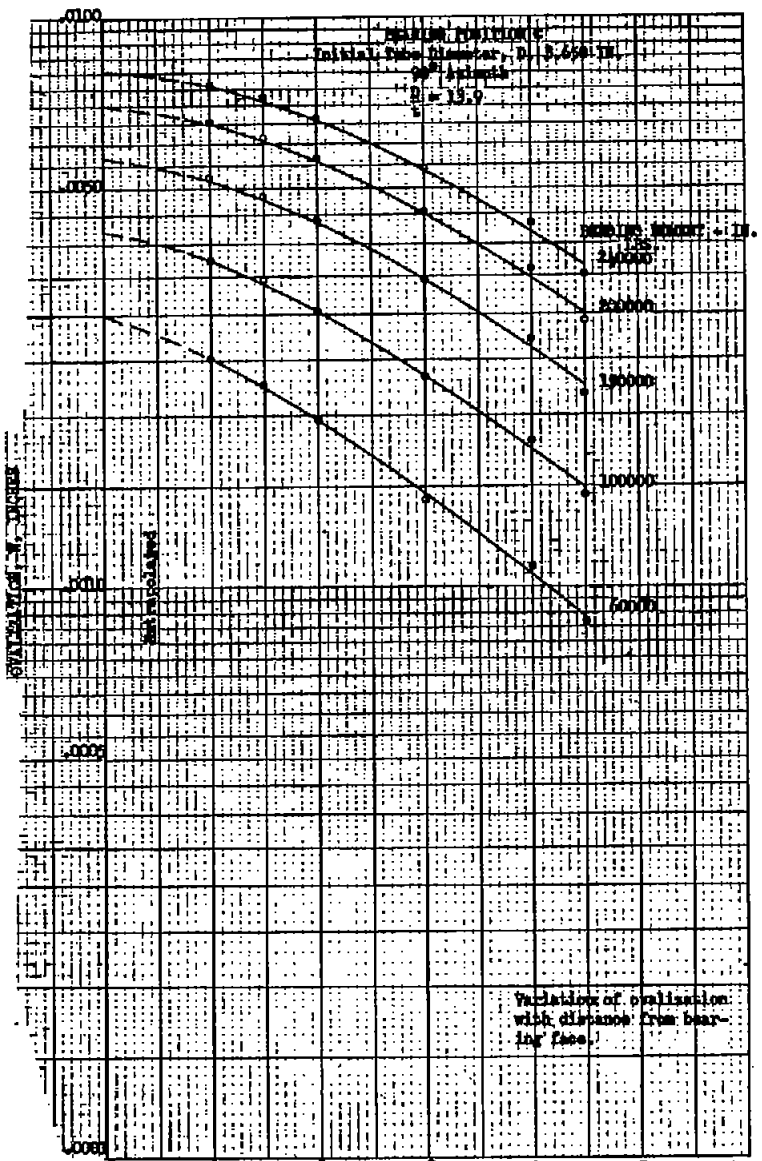

Figure 29

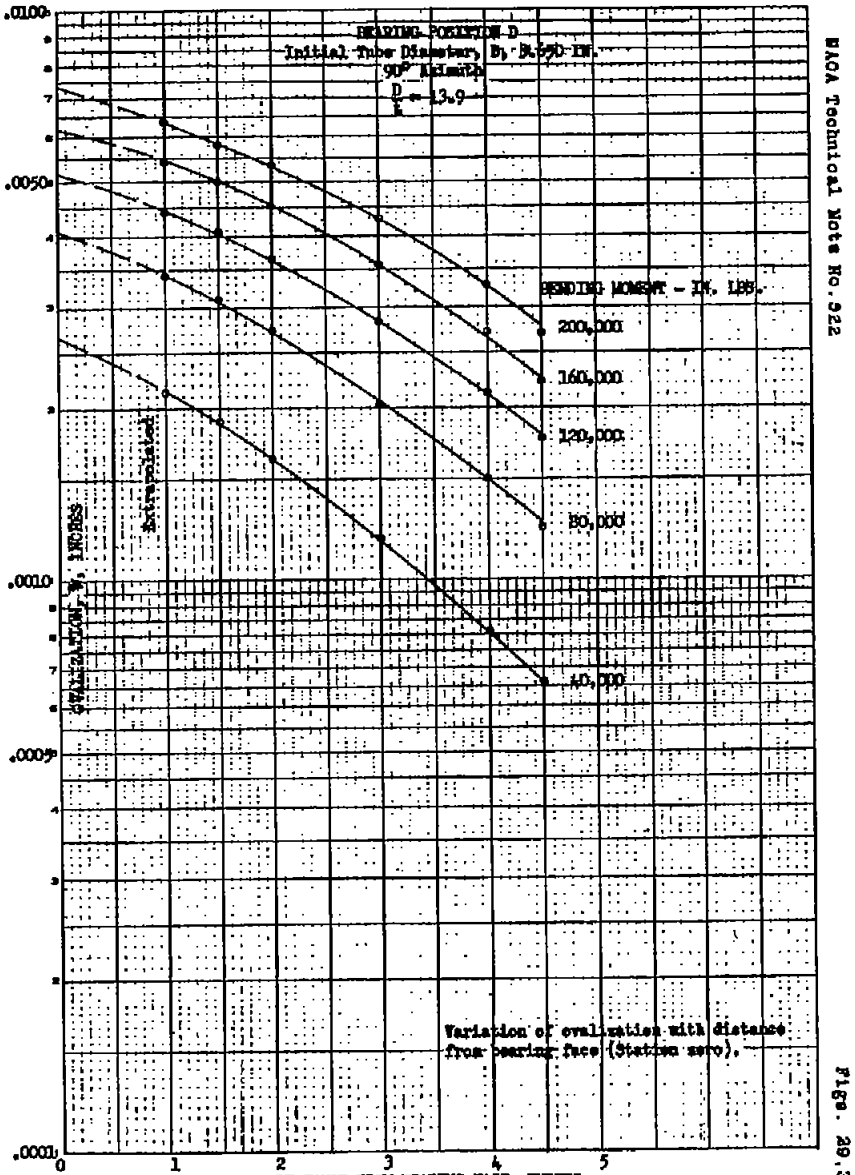

Figure 30

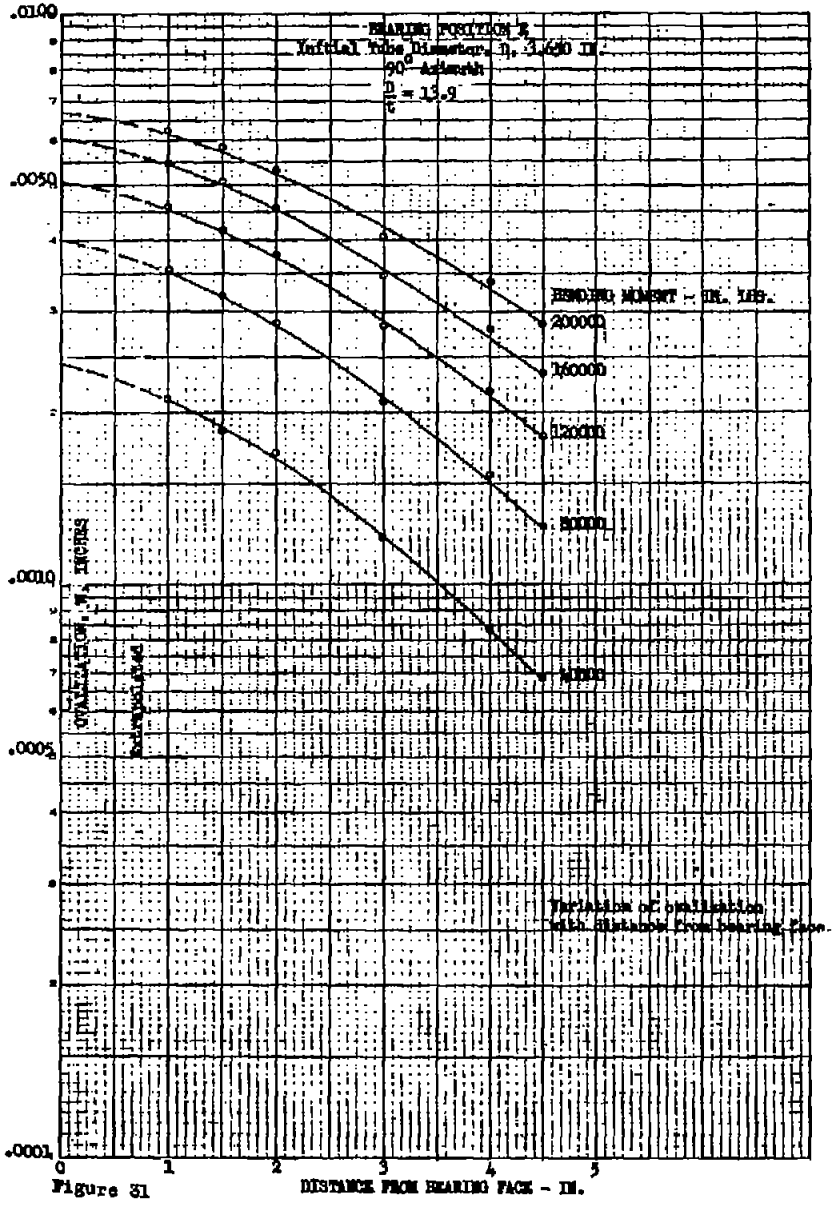

Figure 31

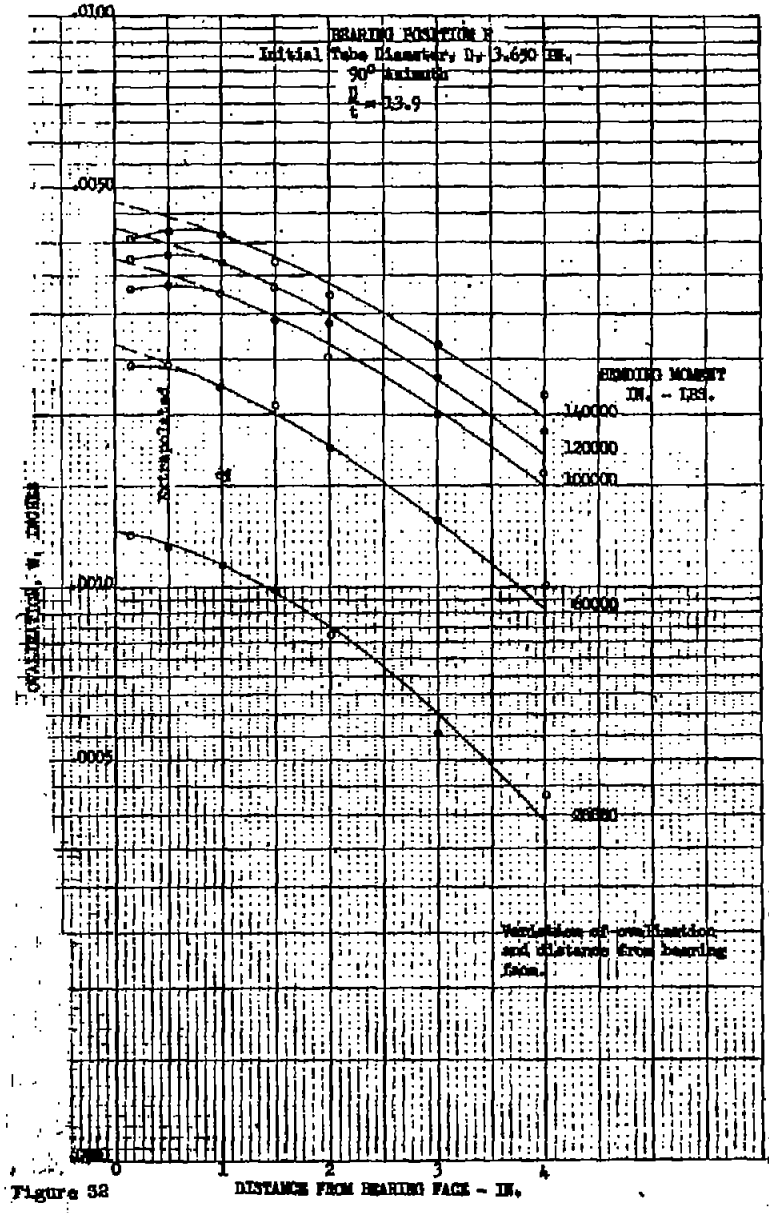

Figure 32

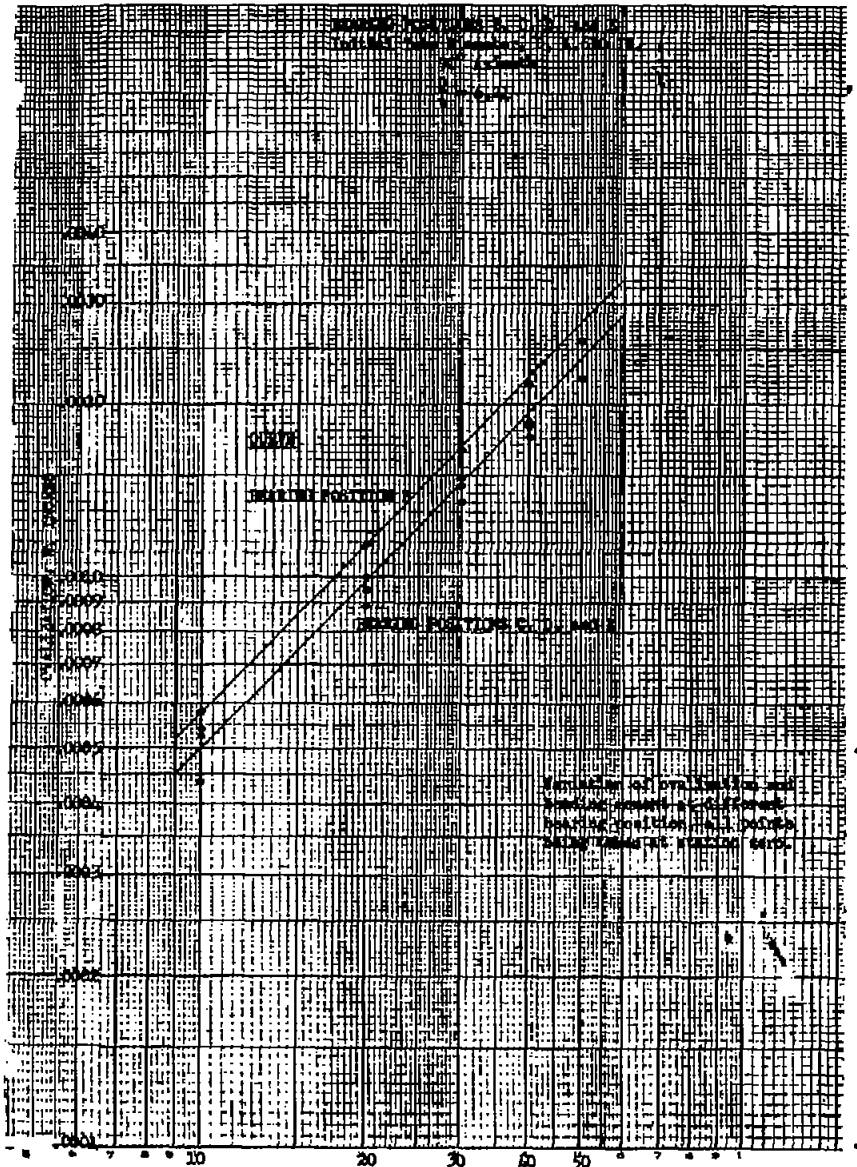

Figure 33

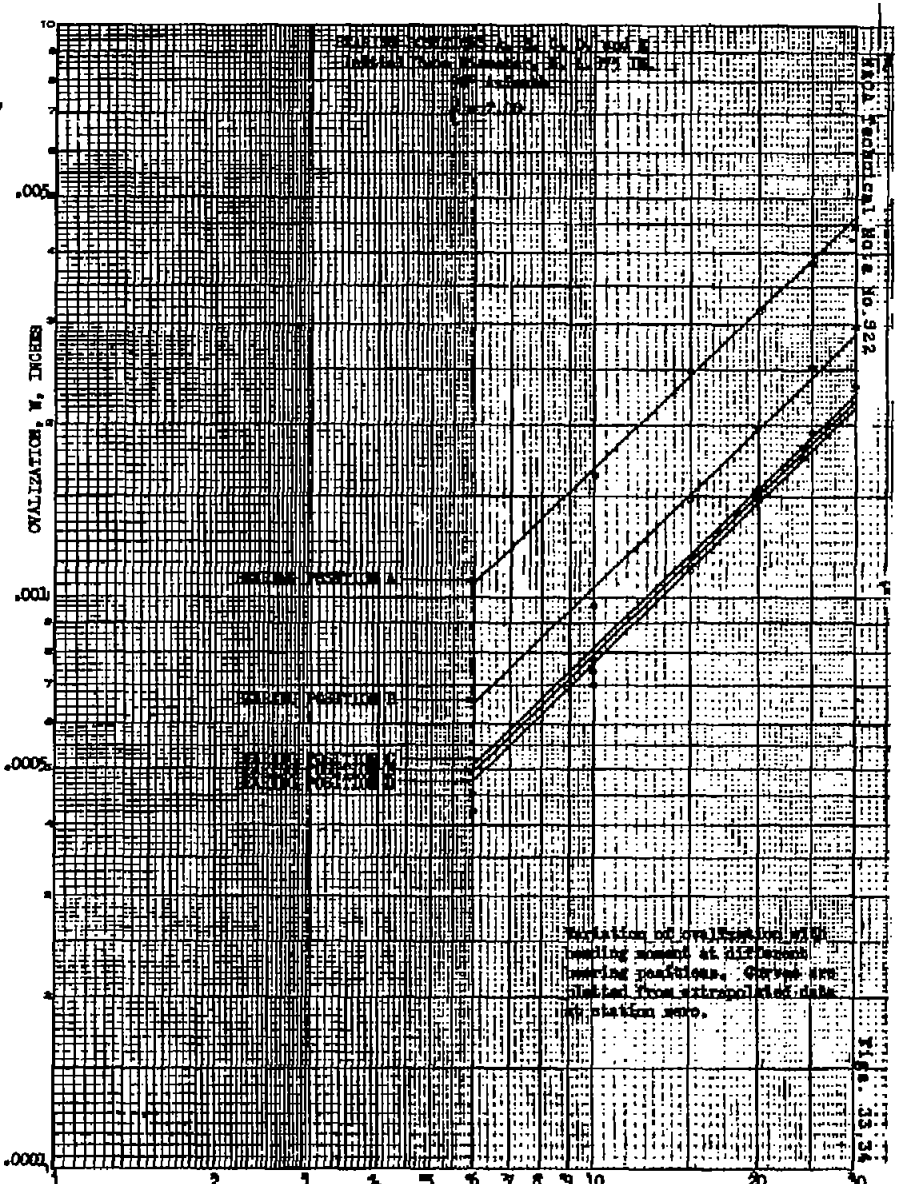

Figure 34

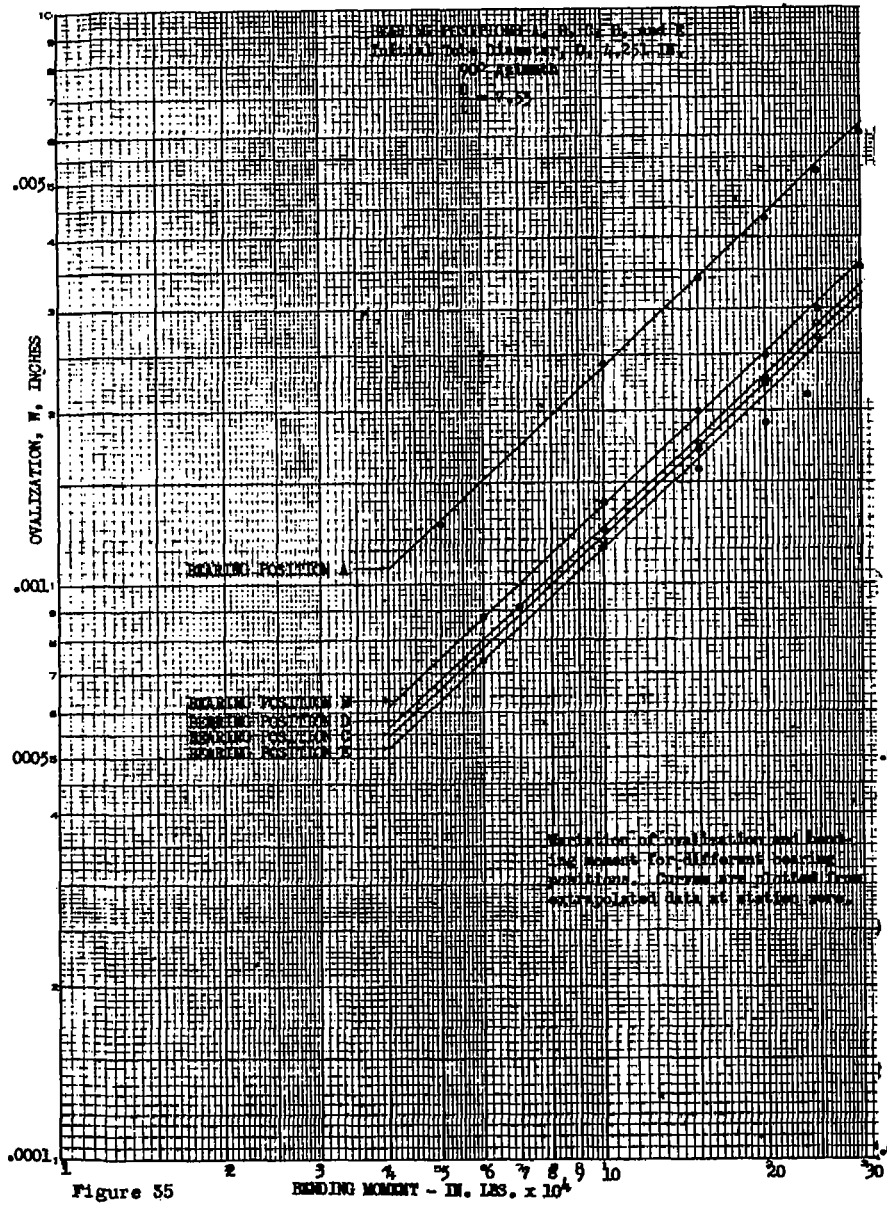

Figure 35

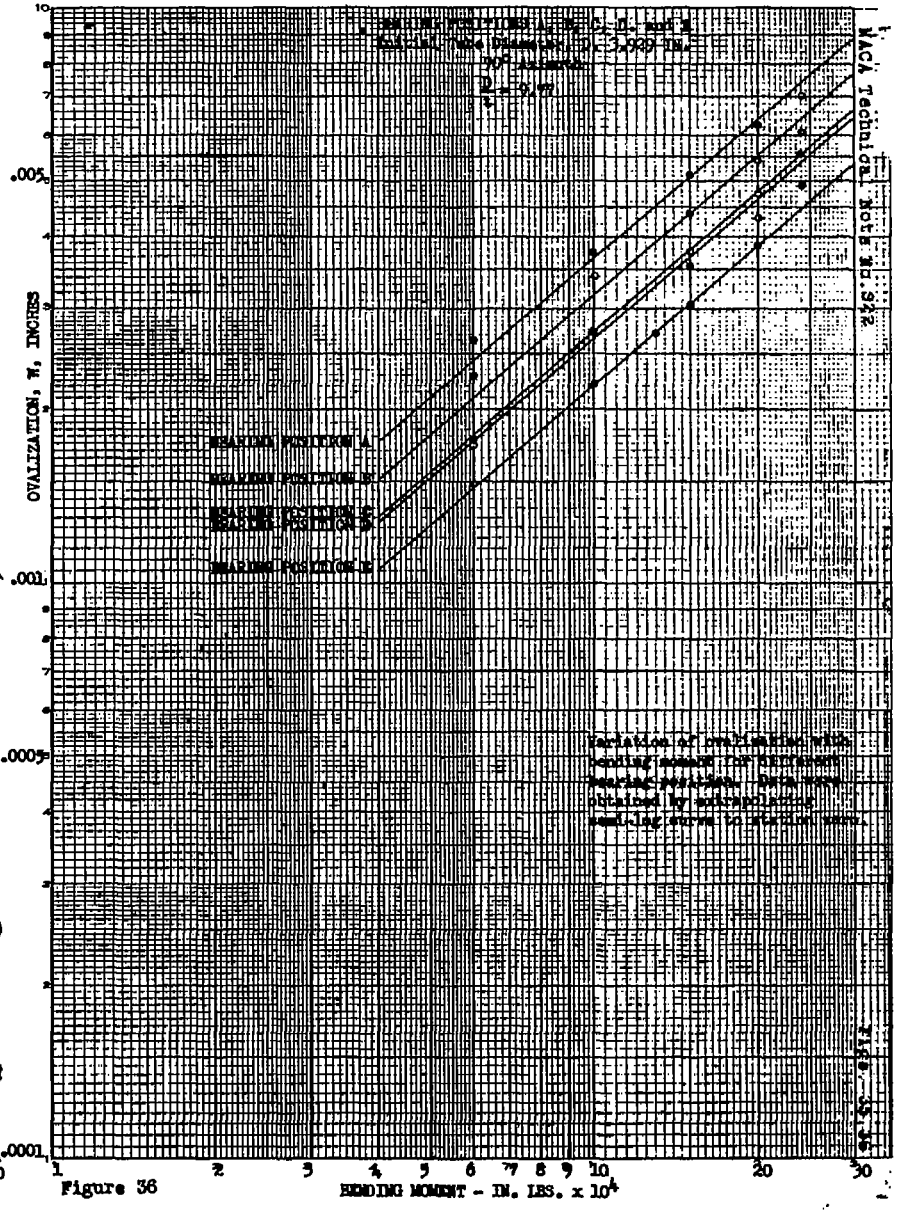

Figure 36

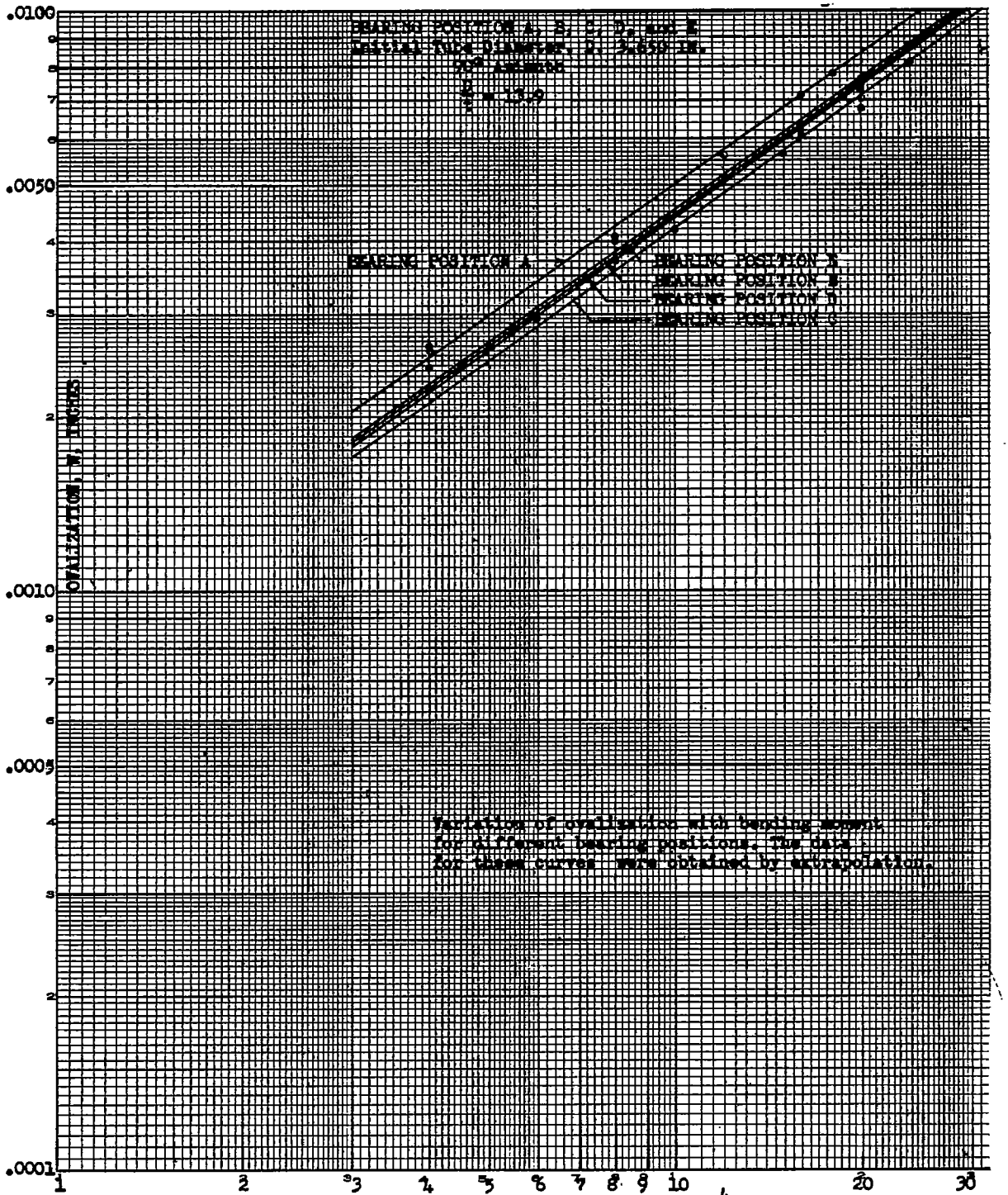

Variation of ovalization with bending moment for different bearing positions. The data for these curves were obtained by extrapolation.

Figure 37

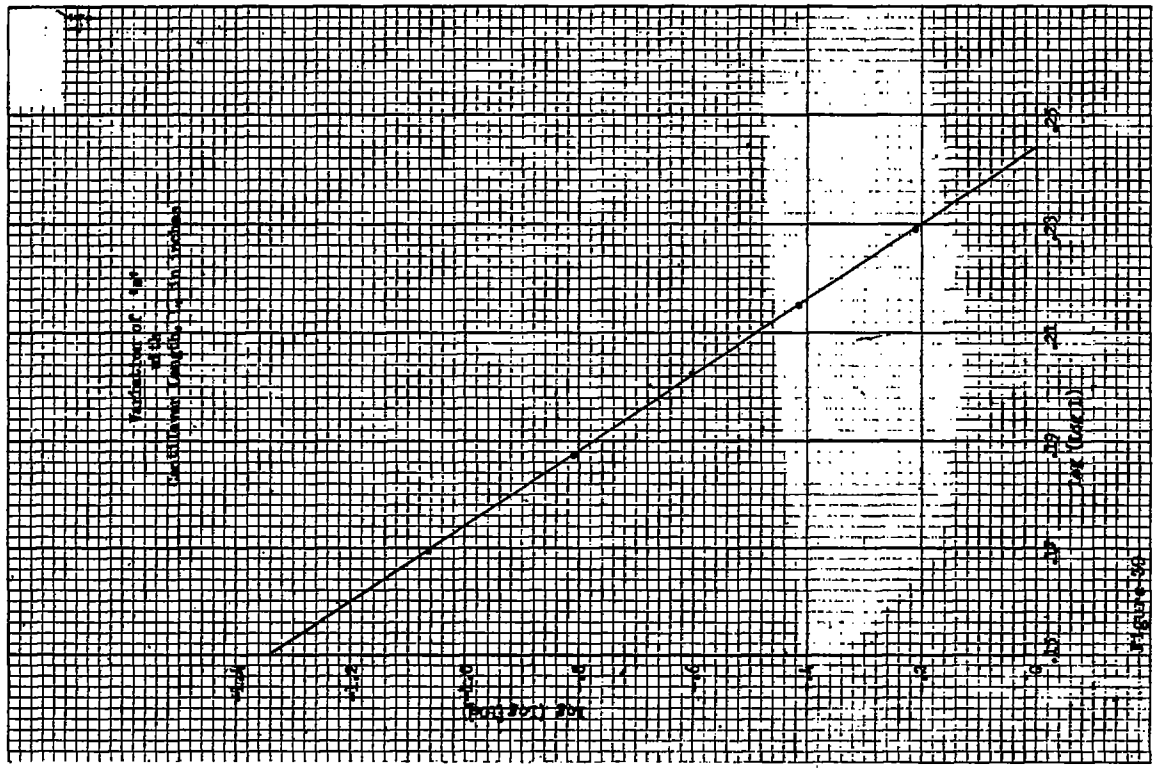

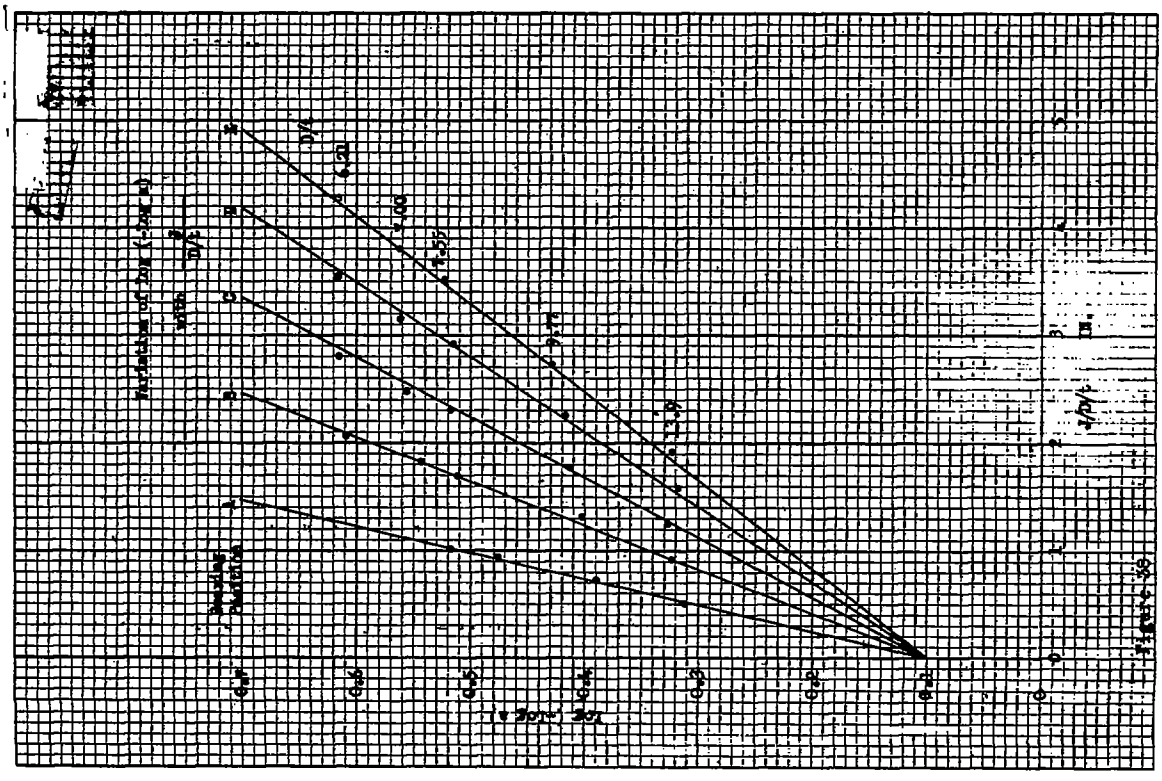

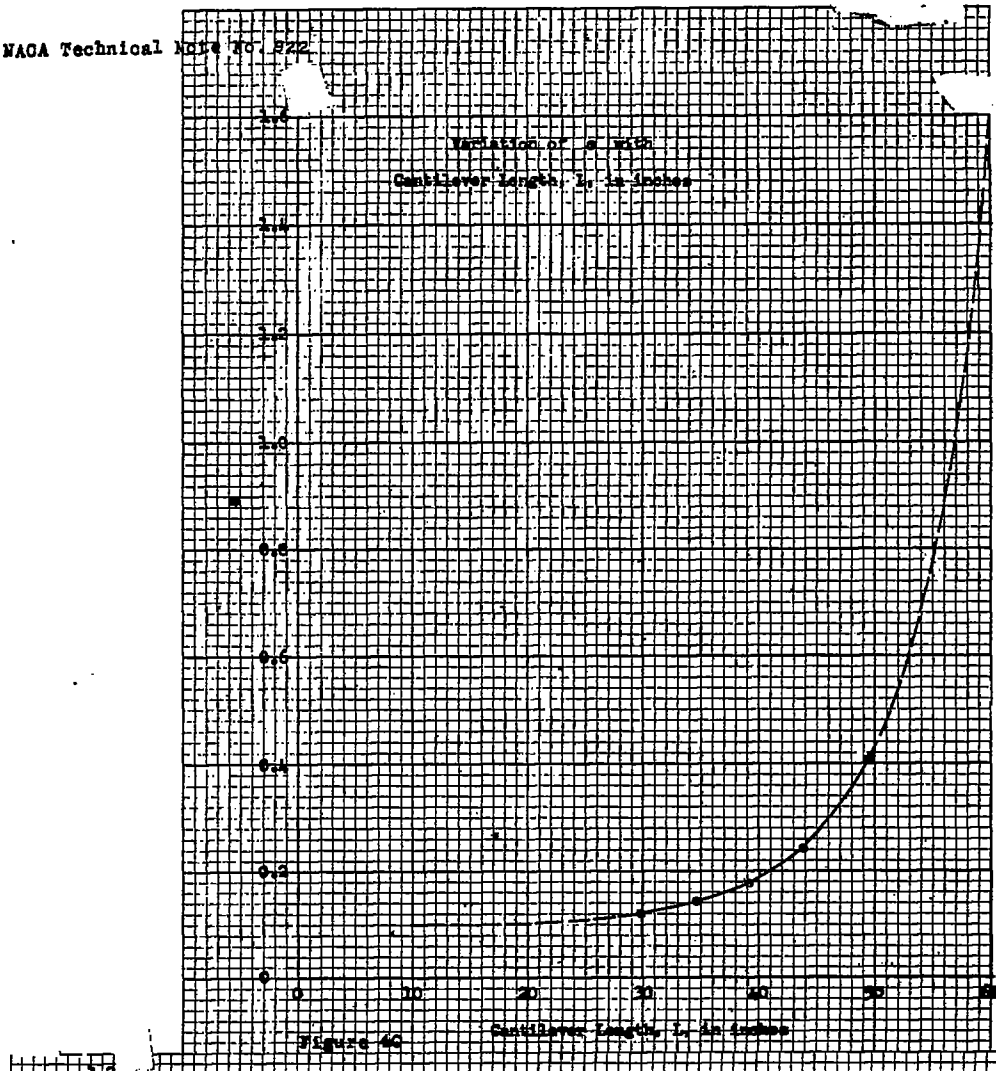

Figure 40

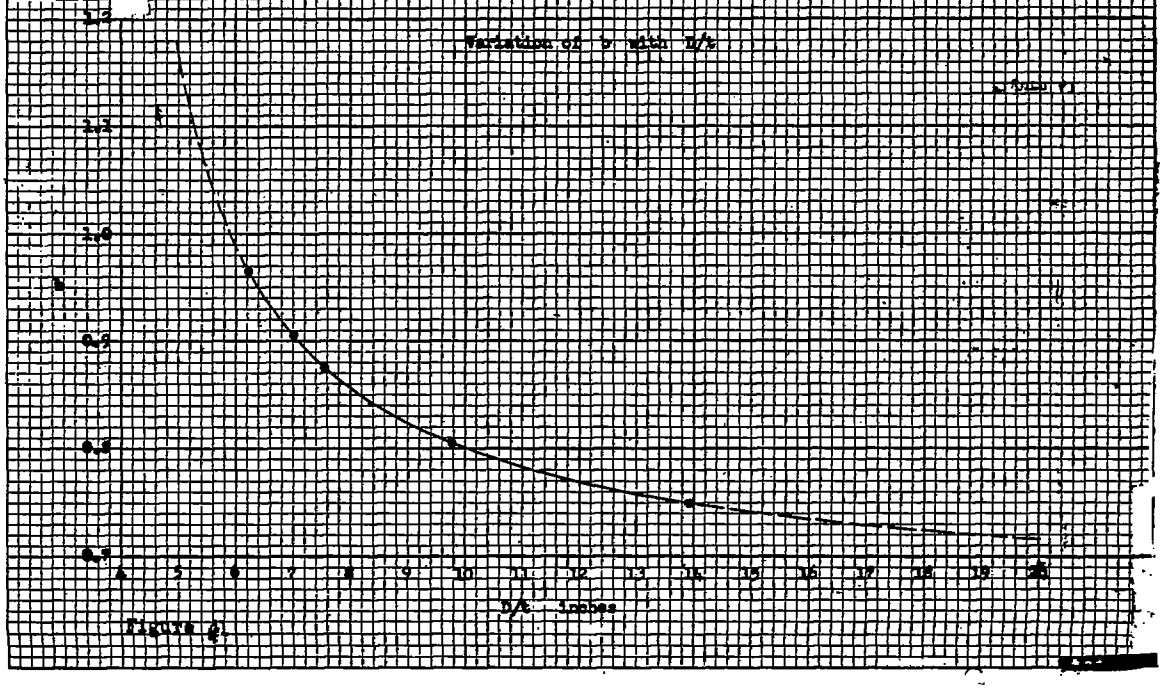

Figure 41